CINDAS

THERMOPHYSICAL PROPERTIES RESEARCH CENTER
ELECTRONIC PROPERTIES INFORMATION CENTER
THERMOPHYSICAL AND ELECTRONIC PROPERTIES INFORMATION ANALYSIS CENTER
UNDERGROUND EXCAVATION AND ROCK PROPERTIES INFORMATION CENTER

SELECTED ELECTRICAL AND THERMAL PROPERTIES OF UNDOPED NICKEL OXIDE

J. E. Keem and J. M. Honig

CINDAS REPORT 52

August 1978

Prepared for

DEFENSE LOGISTICS AGENCY
U. S. Department of Defense
Alexandria, Virginia 22304

CENTER FOR INFORMATION AND NUMERICAL DATA ANALYSIS AND SYNTHESIS
PURDUE UNIVERSITY
PURDUE INDUSTRIAL RESEARCH PARK
2595 YEAGER ROAD
WEST LAFAYETTE, INDIANA 47906

UNCLASSIFIED

SECURITY CLASSIFICATION OF THIS PAGE *(When Data Entered)*

REPORT DOCUMENTATION PAGE		READ INSTRUCTIONS BEFORE COMPLETING FORM
1. REPORT NUMBER	2. GOVT ACCESSION NO. AD-A128 900	3. RECIPIENT'S CATALOG NUMBER
4. TITLE *(and Subtitle)* SELECTED ELECTRICAL AND THERMAL PROPERTIES OF UNDOPED NICEL OXIDE		5. TYPE OF REPORT & PERIOD COVERED State-of-the-Art Report
		6. PERFORMING ORG. REPORT NUMBER CINDAS REPORT 52
7. AUTHOR(s) J. E. Keem and J. M Honig		8. CONTRACT OR GRANT NUMBER(s) DSA900-77-C-3758
9. PERFORMING ORGANIZATION NAME AND ADDRESS Thermophyscial and Electronic Properties Information Analysis Center, CINDAS/Purdue Univ. 2595 Yeager Rd., W. Lafayette,IN 47906		10. PROGRAM ELEMENT, PROJECT, TASK AREA & WORK UNIT NUMBERS
11. CONTROLLING OFFICE NAME AND ADDRESS Defense Technical Information Center,Defense Logistics Agency, Attn: DTIC-AI, Cameron Station, Alexandria, VA 22314		12. REPORT DATE August 1978 13. NUMBER OF PAGES 78
14. MONITORING AGENCY NAME & ADDRESS*(if different from Controlling Office)* Army Materials and Mechanics Research Center Attn: DRXMR-P Arsenal Street Watertown, MA 02172		15. SECURITY CLASS. *(of this report)* Unclassified 15a. DECLASSIFICATION/DOWNGRADING SCHEDULE N/A

16. DISTRIBUTION STATEMENT *(of this Report)*

Distribution unlimited.

17. DISTRIBUTION STATEMENT *(of the abstract entered in Block 20, if different from Report)*

18. SUPPLEMENTARY NOTES

TEPIAC Publication (DTIC Source Code 413571);
Microfiche copies available from DTIC

19. KEY WORDS *(Continue on reverse side if necessary and identify by block number)* *Nickel Oxide--
*Electrical Resistivity--*Seebeck Coefficient--*Heat capacity--
*Thermal Conductivity --*Thermal Expansion--*Elastic Constants

20. ABSTRACT *(Continue on reverse side if necessary and identify by block number)*

This report reviews the recorded world knowledge on the electrical and thermal properties of undoped nickel oxide in a most comprehensive and detailed form making it possible for all users of the subject to have access to the original data without having to duplicate the laborious and costly process of literature search and data extraction. Furthermore, for the active researchers in the field, a detailed discussion is presented for each property, reviewing the available information together with the considerations used by the authors in arriving at the final recommended reference values.

DD FORM 1 JAN 73 1473 EDITION OF 1 NOV 65 IS OBSOLETE

UNCLASSIFIED

SECURITY CLASSIFICATION OF THIS PAGE *(When Data Entered)*

SELECTED ELECTRICAL AND THERMAL PROPERTIES OF UNDOPED NICKEL OXIDE

J. E. Keem and J. M. Honig

Departments of Physics and Chemistry
Purdue University
West Lafayette, Indiana 47907

CINDAS REPORT 52

August 1978

Prepared for

DEFENSE LOGISTICS AGENCY
U.S. Department of Defense
Alexandria, Virginia 22304

CENTER FOR INFORMATION AND NUMERICAL DATA ANALYSIS AND SYNTHESIS
Purdue University
Purdue Industrial Research Park
2595 Yeager Road
West Lafayette, Indiana 47906

PREFACE

This technical report was prepared by the Thermophysical and Electronic Properties Information Analysis Center (TEPIAC), a Department of Defense Information Analysis Center. This Center is operated by the Center for Information and Numerical Data Analysis and Synthesis (CINDAS), Purdue University, West Lafayette, Indiana, under Contract No. DSA900-77-C-3758 with the Defense Logistics Agency (DLA), Alexandria, Virginia, with Mr. J.L. Blue (Hq. DLA) as the IAC Program Manager and Mr. Samuel Valencia (Army Materials and Mechanics Research Center) as the Contracting Officer's Technical Representative.

The report was authored by Dr. John E. Keem, who held a joint appointment in the Department of Physics and Department of Chemistry of Purdue University, and Dr. J.M. Honig, Professor of Chemistry at Purdue. Dr. Keem's present address is: Physics Department, General Motors Technical Center, General Motors Corporation, Warren, Michigan 48090. It was under a collaborative working arrangement between the two authors and CINDAS that this technical report was produced.

This report reviews the recorded world knowledge on the electrical and thermal properties of undoped nickel oxide in a most comprehensive and detailed form making it possible for all users of the subject to have access to the original data without having to duplicate the laborious and costly process of literature search and data extraction. Furthermore, for the active researchers in the field, a detailed discussion is presented for each property, reviewing the available information together with the considerations used by the authors in arriving at the final recommended reference values.

It is hoped that this work will prove useful not only to the scientists in the field but also to engineering research and development programs and for industrial applications, as it provides a wealth of knowledge heretofore unknown or inaccessible to many. In particular, it is felt that the critical data evaluation and analysis and reference data generation constitute a unique aspect of this work.

Y. S. TOULOUKIAN
Director of CINDAS
Distinguished Atkins Professor
of Engineering
Purdue University

August 1978
West Lafayette, Indiana

TABLE OF CONTENTS

1. INTRODUCTION

The objective of this project was to compile, critically evaluate, and analyze available data and information on the dc electrical resistivity, Seebeck effect (thermoelectric power), heat capacity at constant pressure, thermal and elastic properties of single crystal, polycrystalline, and annealed specimens of pure NiO in the temperature range of kinetic stability, and finally, to generate recommended reference values for selected properties of different forms of NiO.

Section 2 provides certain necessary background information. Section 3 presents experimental data in graphical and tabular forms along with the critically evaluated and recommended values for dc electrical resistivity, Seebeck coefficient, heat capacity (at constant pressure), thermal conductivity, elastic properties, and thermal expansion. Also included in these sections is explanatory information for each property, on the basis of which the available data are reviewed and discussed. Statements are also provided concerning criteria and considerations used in obtaining the recommended values, over the temperature range of kinetic stability. The (provisionally) recommended values of various properties are exhibited along with the experimental data. The complete bibliographic citations for the references are given in Section 4.

It should be carefully noted that we exclude from this report a considerable body of data pertaining to the properties of NiO above 1000 K or of doped NiO, including particularly Li-doped NiO, since the properties of these materials are not representative of pure NiO at ordinary temperatures.

2. GENERAL BACKGROUND

2.1 Physical Characteristics

Above 523 K NiO is an anion excess, paramagnetic material in the cubic rocksalt configuration with one molecule per primitive cell; the lattice constant is 4.1811 Å.[1] Below the Néel temperature of T_N = 523 K, NiO is a type 2 antiferromagnet,[2] with a slight rhombohedral lattice distortion [0.15% contraction along a (111) axis] caused by magnetostriction.[3] The compound exhibits small deviations from strict stoichiometry, representable by the formula $Ni_{1-\delta}O$, with deviations in the range $0 \leq \delta < 5x10^{-3}$. As δ is decreased by appropriate annealing[4] from its upper limit towards zero NiO transforms from a black opaque material, which may have a greenish cast, to a green translucent material. The resistivity at fixed temperature is increased many orders of magnitude as the material is rendered increasingly stoichiometric.

A striking feature of crystalline NiO is the inertness of this material toward chemical changes. Reduction to metallic Ni can only be achieved by heating under almost total exclusion of oxygen ($P_{O_2} < 10^{-20}$ atm) or by use of hydrogen at elevated temperatures. NiO can be dissolved only in molten salts such as $K_2S_2O_7$. Acids and bases have no noticeable effect on the properties of crystalline NiO. The density of NiO at room temperature is 7.45 gm/cm^3; its melting point is approximately 2230 K.

Single crystals of NiO may be prepared by at least five different techniques involving high temperature methods: flame fusion (also termed the Verneuil technique),[5] arc image furnace floating zone,[6] plasma torch,[7] solar furnace melting technique, [8] and arc-transfer.[9] Three others, halide decomposition and deposition on MgO substrates,[10] chemical vapor transport,[11] and growth from a flux,[12] are carried out at much lower temperatures. No measurements have so far been reported on NiO grown by chemical vapor transport.

Typically, samples obtained by the high temperature techniques are more strained and nonstoichiometric than those grown by halide decomposition, though halide-decomposition-grown specimens also exhibit strain caused by the mismatch between the MgO substrate and NiO lattice. It is possible, however, by annealing to improve the stoichiometry and to reduce internal strains to the point where the samples so treated become superior to the thin film material grown by halide decomposition. In general the electrical transport properties of NiO are much altered by changing the state of internal strain and degree of stoichiometry, whereas heat capacity and elastic properties seem less sensitive to these parameters. The critical evaluation of particular data with regard to these factors will be discussed in the following subsections, along with the general background information relevant to each set of experimental data.

2.2 DC Electrical Resistivity

Electrical resistivity measurements in transition metal oxides suffer from two classes of problems: those related to material quality (including thermal history) and those connected with measurement techniques.

The presence of voids and other crystal defects alters, both in quality and degree, the electrical conductivity in NiO. Empirically, it is found that fused polycrystalline material composed of macroscopic single crystal domains exhibit electrical transport properties very similar to those of single crystals. By contrast, sintered ceramic specimens show resistivity variations which cannot be simply associated with a decrease number of conducting paths due to the presence of voids. The details of these alterations depend on the sintering process such as the firing schedules, the firing atmosphere, and the compaction techniques. Further, different sintering processes produce various

types of internal boundaries and surfaces whose electrical conduction characteristics are in general different from those of the interior of the grain. Depending on the relative magnitudes of the surface and bulk conductivities, the electrical characteristics of one may overshadow that of the other and thus, lead to wide differences in observed characteristics. In addition, prolonged exposure to elevated temperatures during sintering may also inadvertently allow substantial amounts of impurities to diffuse into the material where their effects are sometimes compounded by the proclivity of certain cations to segregate on grain boundaries and at other defect sites.

Because of the ambiguity introduced by the sintering process, recommended resistivity values for ceramic specimens should be regarded with circumspection, because such measurements cannot be reliably reproduced. Electrical conductivity data for polycrystalline and single crystal specimens are relatively more uniform and reproducible in characteristics.

After the state of aggregation the next most important materials parameter is the past thermal history of the samples. Whenever single crystals of NiO are heated above approximately 1000 K[13] solid state reactions begin to occur on laboratory time scales. These reactions first involve equilibration of surface defects with the ambient oxygen partial pressure; also, changes occur which reduce the extent of high strain regions on the surfaces of the specimen. Above 1300 K[13] these processes begin to produce changes in bulk stoichiometry and give rise to relief of internal strain. Since charge transport occurs by motion of carriers (holes) which arise from the presence of cation defects (Ni^{+2} vacancies) it is evident why various heat treatments under different atmospheres cause tremendous changes in the electrical resistivity of a sample. Hence, a major concern of this report is a careful, critical

analysis of the data acquired from similar specimens with different thermal histories.

As concerns measurement techniques, it is important to note that the specimens in pure form have resistivities considerably in excess of 10^6 ohm-cm at temperatures below the Néel point T_N = 523 K. Electrical measurements in this temperature region require the use of very high input impedance devices such as electrometers, varactor bridge operational amplifiers, or FET input operational amplifiers for voltage sensing.[14] These precautions are particularly crucial in the measurement of Seebeck coefficients. Resistivities should always be determined by the standard four-probe technique to avoid complication due to junction impedances. Unless these precautions are taken electrical measurements at best are suspect and at worst,meaningless. In the data evaluations at later Sections an attempt has been made to take these various factors into account.

2.3 Seebeck Coefficient (Thermoelectric Power)

The Seebeck effect in a material is due to the production, under steady state heat flow and zero electrical current flow conditions, of a small gradient in electrochemical potential as the result of the imposition of a small temperature gradient. The magnitude of the effect is specified by the Seebeck coefficient*, $\alpha = \Delta V/\Delta T$, i.e., by the voltage difference per unit temperature difference across the sample, measured at a specified average sample temperature.[15] The variation of α as a function of temperature,

*Strictly speaking, $\alpha \equiv \nabla(\zeta/e)/\nabla T$, where ζ/e is the electrochemical potential per unit electronic charge, and ∇ is the gradient operator, but for most cases this rigorous definition reduces to the one shown above.

in conjunction with a model for the electronic states in the material, provides information on the magnitude and temperature dependence of the carrier density and on the degree of electron-lattice and/or electron-magnon coupling.[16]

The experimental difficulties encountered in electrical measurements also have their counterparts in Seebeck coefficient measurements. Earlier remarks regarding sample quality are applicable to the present situation, particularly since Seebeck coefficients of different parts of a sample (e.g., surfaces and grains in sintered compacts) are weighted by the conductivity σ_i of that portion of the sample, relative to the total conductivity, σ_T. The overall Seebeck coefficient is given by

$$\alpha_T = \sum_i \alpha_i \frac{\sigma_i}{\sigma_T} \qquad (1)$$

where the summation i is taken over all different types of charge carriers which may be identified as contributing to the overall transport properties of the material.

Special difficulties are associated with Seebeck effect measurements and their interpretation in very high resistivity materials.[14] These arise from the need to measure the small magnitudes of the Seebeck voltages, typically a few millivolts or less, on specimens whose total resistance may be in excess of 10^{12} ohms for pure samples of NiO. Further, the accurate imposition of a small temperature gradient without disturbing the sample is a difficult, though important task. In general, the use of buffering circuitry for isolating the sample, and employing special predictive filtering techniques for optimizing the signal-to-noise ratio, as well as the use of nonelectrical

methods for imposing the temperature gradients with a four-probe technique are essential to obtain meaningful results on high resistivity specimens. The delicacy of such measurements frequently has not been sufficiently appreciated.

2.4 Heat Capacity (At Constant Pressure)

One of the most fundamental thermodynamic measurements which can be executed on any material is the determination of its heat capacity at constant pressure, C_p. Evaluation of the integrals $\int_0^T C_p \, dT$ and $\int_0^T T^{-1} C_p \, dT$ yield the enthalpy and entropy, respectively of the material under study, and from the latter two quantities the Gibbs free energy of the compound may be evaluated.

To compare experimental measurements with theory, it is necessary to convert to the heat capacity at constant volume, C_V, via the expression

$$C_p = C_V + \alpha_I^2 VT/\beta \qquad (2)$$

wherein α_I is the coefficient of thermal expansion for NiO,[17] β its compressibility,[18] T the temperature, and V, the volume. According to the Debye theory of lattice vibrations in solids, C_V is expected to approach asymptotically the limiting Dulong and Petit value of 3nR at high temperature, where R is the gas constant and n the number of atoms in the formula unit. Heat capacity measurements in NiO are subject to an additional complication: near 523 K the material undergoes a magnetic disordering transition in converting, on heating, from an antiferromagnetic to a paramagnetic insulator. In accordance with well-known theories of order-disorder transitions,[19] this gives rise to the so-called lambda-type anomaly in the heat capacity, i.e., a broad peak terminating in a rather abrupt spike, superposed on a normally rising background.

As already mentioned, these measurements are expected to be rather insensitive to methods of sample preparation, thermal history, or state of aggregation of the material.

2.5 Thermal Conductivity

The thermal conductivity of a solid depends on the degree of aggregation if it is ceramic, and on the direction of heat flow with regard to crystallographic axes if it exhibits crystalline anisotropy. In a magnetically ordered crystalline material such as NiO, an additional dependence of the thermal conductivity on the degree of magnetic order is also observed.[20] These magnetic effects are obscured in ceramic specimens due to the random orientations of the magnetic axes; in other respects, above room temperature the thermal conductivity of ceramic specimens is closely proportional to that of single-crystal material. In this regime the mean free path of phonons is small compared to the average distance between defects, and the magnitude of the thermal conductivity is governed solely by the porosity of the specimens: voids of any type may be considered to function as very high thermal resistances. It is only at lower temperatures, where the phonon mean free path becomes large, that the correlation between thermal conductivity of single crystal and ceramic specimen breaks down. Phonons then scatter off the macroscopic defects such as dislocations, voids, grain boundaries, magnetic domain, internal strains, and the like.

To determine the intrinsic lattice and magnetic contributions to the thermal conductivity, it is clearly necessary to rely exclusively on measurements performed on single crystals of the highest quality. Even so, the need for thermal shielding to avoid spurious heat transport by extraneous conditions and radiation, makes it difficult to obtain reliable data.[20,21] It should

be kept in mind that radiation effects are proportional to the fourth power of the temperature difference between the specimen and the surroundings, and therefore, particularly troublesome.

2.6 Elastic Constants

Because the electrical conduction in this material seems to be closely linked to the elastic properties of the crystal,[22] precise values for the elastic coefficients and their variation with temperature are of considerable fundamental interest, as well as being important in determining the possible technological uses of this material. Measurement of elastic coefficients using low frequency ultrasound (10^7 hz) are relatively unaffected by the state of sample subdivision so long as the density is close to that of the ideal material. An alternative method consists in determining phonon dispersion curves from inelastic neutron scattering. Data using both types of techniques are cited in Sec. 3. All elastic constants normally are weakly dependent on temperature; however, one anticipates rather drastic changes in these quantities and in Young's modulus as the material passes through the magnetic ordering temperature.

2.7 Coefficients of Thermal Expansion

Thermal expansion is usually monitored by dilatometric techniques or by direct optical studies. On occasion, X-ray diffraction experiments have been utilized to determine the variation of lattice parameters with temperature, and the coefficient of thermal expansion is then calculated from these data. All three techniques have been utilized in the determinations cited in Sec. 3. These studies are not very sensitive to departures from stoichiometry,

but they are dependent on the availability of specimens with relatively low porosity.

2.8 Data Analysis and Further Comments

The Hall effect, normally an important part of any study of electrical transport properties, is not considered in this report. This omission is justified on three grounds: First, there are very few reports of the Hall effect on single crystals; thus, no real basis for critical evaluation exists. Second, in the few instances where Hall effect is reported, the results are at extreme variance with one another. There is no agreement on such fundamental quantities as the sign, or the sign reversals near the Néel transition, let alone the magnitude of the Hall coefficients, even when measurements are carried out on nominally similar material. Third, in an antiferromagnetic material such as NiO where hopping conduction may dominate (see Sec. 3.2), the theoretical basis for interpreting, and hence, for generating recommended values of the Hall effect are exceedingly complex.[23] Moreover, the predictions vary, depending on the precise model and on the particular charge carrier transport configuration which is assumed.

As regards data evaluation for the remaining transport coefficients, critical analysis and careful comparative evaluation are essential in the generation of reliable recommended values for the thermophysical properties. Procedures for data analysis for single crystals and polycrystalline ceramic specimens are similar. They consisted in assessing, where possible, the validity and reliability of the data, based on description of experimental procedures, related information, and internal consistency. It was further attempted to resolve conflicts and discrepancies in data, to correlate data in light of

various controlling parameters, to carry out curve fitting with theoretical or empirical equations, and to compare results with theoretical predictions or generalized empirical correlations. Theoretical methods and semiempirical techniques have also been employed to fill data gaps so that the resulting recommended values would be internally consistent and cover as wide a range in the relevant controlling parameters as possible. Such analyses were carried out only for those properties on which a considerable selection of data were available.

Considering electrical resistivity, for example, in the evaluation of a particular set of measurements, the temperature dependence of the data was examined and any unusual feature or anomaly carefully investigated. The experimental technique was reviewed to be certain that contact effects, unwanted loading, spurious voltage sources, and inappropriate physical conditions of the measurement are accounted for, and that the samples were carefully prepared in a suitable atmosphere by reliable techniques. Also, as far as possible, estimates of uncertainty were checked to ensure that all sources of error had been considered. Data were considered reliable only if all sources of systematic error had been eliminated, or minimized and accounted for.

The selected sets of data were classified according to values of important controlling parameters, and recommended or provisional values of the electrical resistivity were generated for each value of the controlling parameters. For unannealed single crystals, a theoretical curve is available and is compared with the appropriate data over the temperature range for which the theory is considered valid.

3. PRESENTATION OF DATA

Each of the subsections shown below deals with data pertinent to undoped single crystal or polycrystal specimens of Nickel Oxide. The experimental results are exhibited in graphical and in tabular form, along with information covering sample preparation and measurement techniques. In addition, where possible, we have generated sets of recommended values for the property under consideration. These are entered in graphical form on the various figures; representative numerical values read off from these smoothed graphs are entered separately in appropriate tables.

One should recognize that the electrical prorerties are very sensitive to departures from the ideal 1:1 ratio of O/Ni; hence in resistivity and Seebeck coefficient measurements, distinctions have been made between samples of different stoichiometry by referring to $Ni_{1-\delta}O$, with $0 \leq \delta \lesssim 5 \times 10^{-3}$. The mechanical and thermal properties are far less sensitive to these effects; consequently, the distinction has been dropped in later sections and all samples have been designated simply as NiO.

3.1 Electrical Resistivity

Recommended values for the resistivity of undoped single crystal specimens of $Ni_{1-\delta}O$ in the range of its kinetic stability are shown in Table 1. The procedure for obtaining these values is discussed in Sec. 3.2. The results of resistivity measurements are displayed as plots of log ρ(ohm-cm) vs. $10^3/T(K^{-1})$ in Fig. 1 for single crystals and in Fig. 2 for polycrystalline materials. The temperature range for these investigations extends from ca. 250 K to 1000 K, over which the density of Ni ion vacancies remains constant, being determined

TABLE 1

RECOMMENDED RESISTIVITY VALUES FOR SINGLE CRYSTAL $Ni_{1-\delta}O$ IN THE RANGE OF ITS KINETIC STABILITY

Temperature, K	ELECTRICAL RESISTIVITY, ohm-cm		
	Nearly Stoichiometric Sample A	Partially Annealed Sample B	Unannealed Sample C
2000	—	3.34	—
1430	—	—	9.00×10^{-1}
1330	—	1.75×10^{1}	—
1110	2.04×10^{2}	—	—
1000	2.41×10^{2}	4.56×10^{1}	1.30
910	4.13×10^{2}	—	—
800	5.00×10^{3}	9.10×10^{1}	1.92
670	2.15×10^{5}	2.00×10^{2}	3.30
570	4.65×10^{6}	6.15×10^{2}	7.28
500	7.18×10^{7}	3.95×10^{3}	2.08×10^{1}
440	7.84×10^{8}	3.68×10^{4}	9.10×10^{1}
400	7.24×10^{9}	3.23×10^{5}	4.62×10^{2}
360	5.05×10^{10}	2.90×10^{6}	2.47×10^{3}
330	3.45×10^{11}	2.50×10^{7}	1.45×10^{4}
310	1.80×10^{12}	2.18×10^{8}	7.98×10^{4}
290	8.10×10^{12}	1.63×10^{9}	4.10×10^{5}
270	—	1.17×10^{10}	1.94×10^{6}
250	—	8.20×10^{10}	8.20×10^{6}
240	—	5.00×10^{11}	3.43×10^{7}
220	—	2.67×10^{12}	1.38×10^{8}
210	—	1.15×10^{13}	4.95×10^{8}
200	—	—	1.50×10^{9}
190	—	—	3.68×10^{9}
180	—	—	7.00×10^{9}

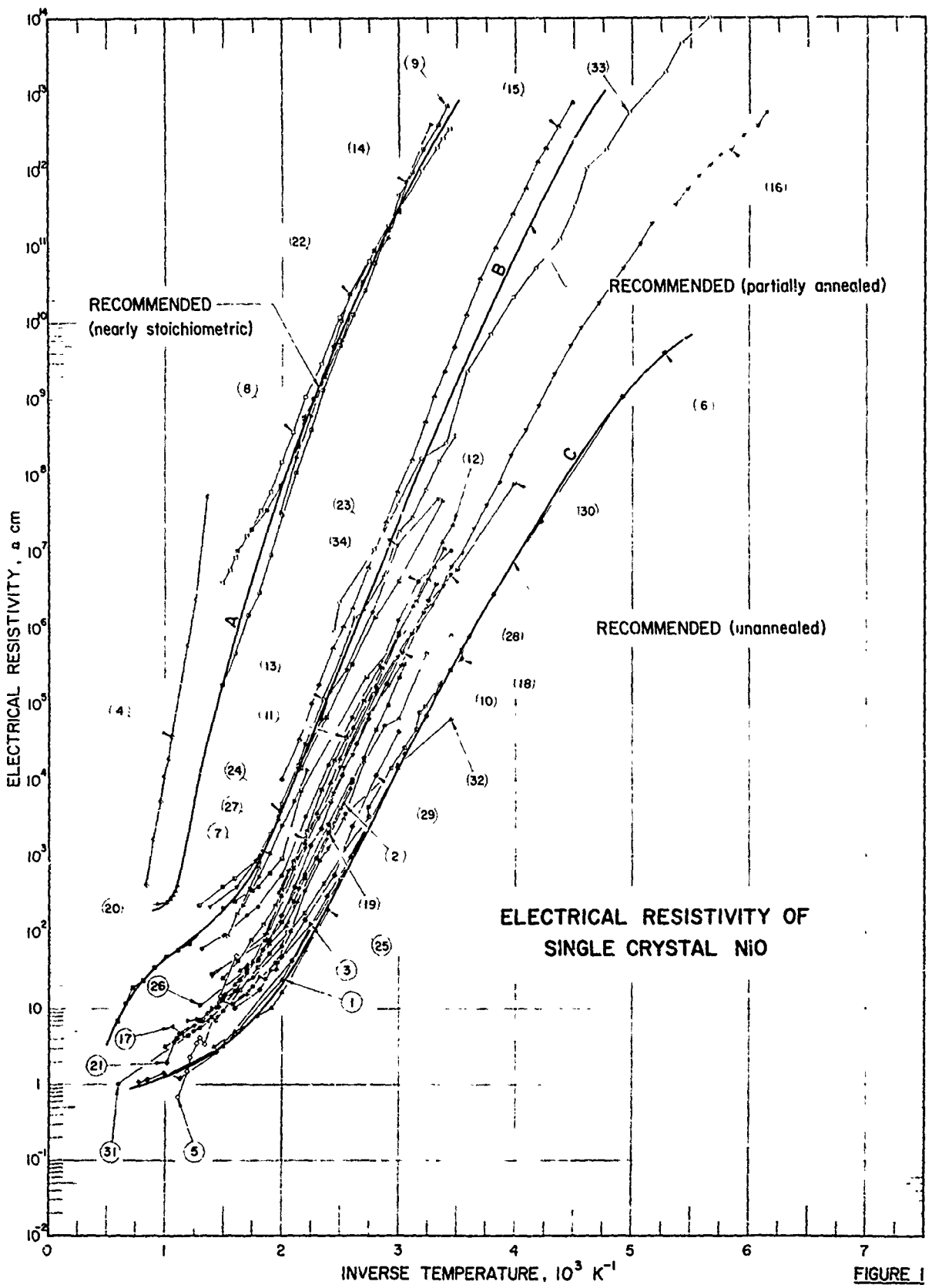
ELECTRICAL RESISTIVITY, Ω cm
INVERSE TEMPERATURE, 10^3 K^{-1}
RECOMMENDED (nearly stoichiometric)
RECOMMENDED (partially annealed)
RECOMMENDED (unannealed)
A
B
C
ELECTRICAL RESISTIVITY OF SINGLE CRYSTAL NiO

FIGURE 1

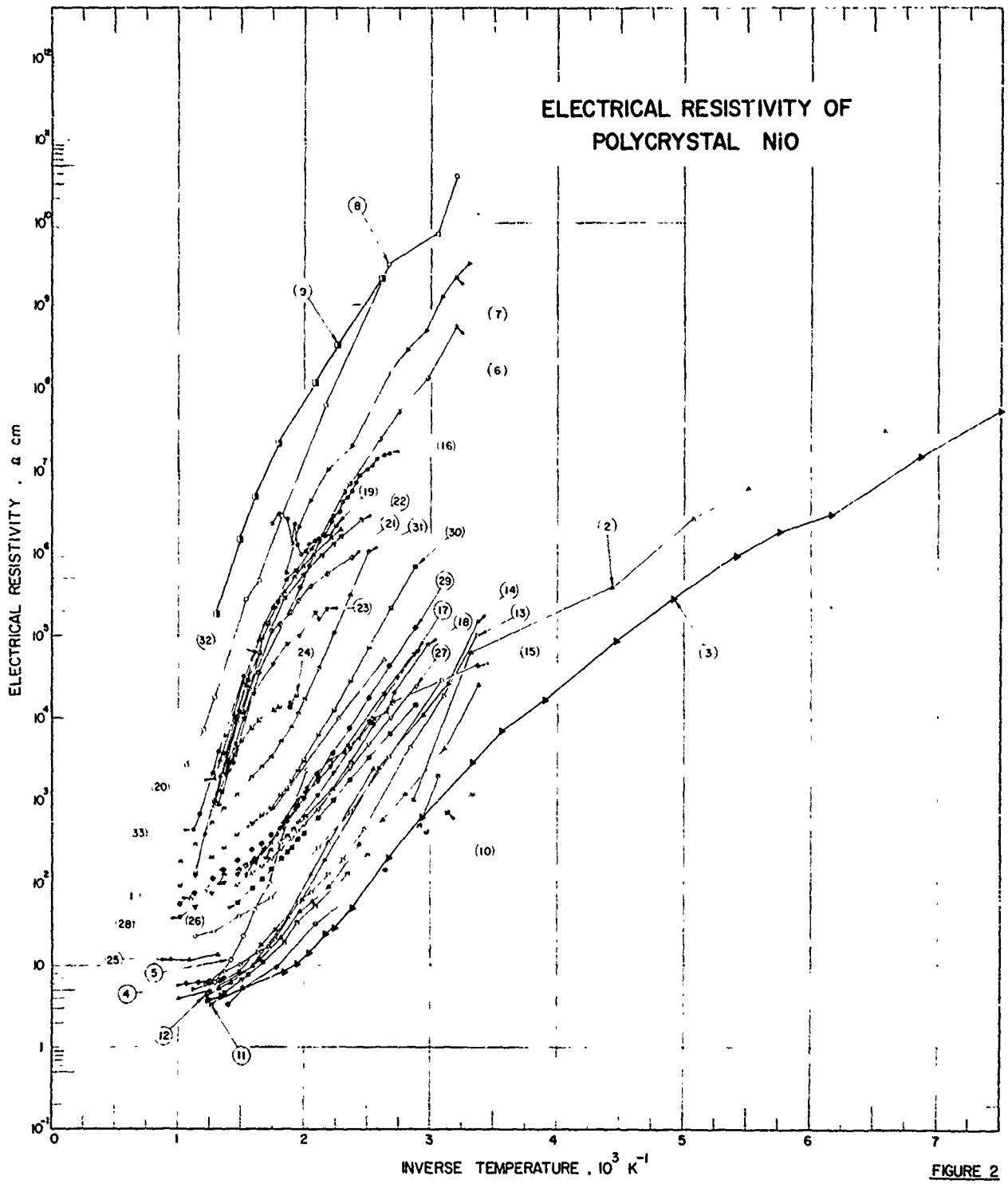
ELECTRICAL RESISTIVITY OF
POLYCRYSTAL NiO
ELECTRICAL RESISTIVITY , Ω cm
INVERSE TEMPERATURE , 10³ K⁻¹
0
1
2
3
4
5
6
7
(1)
(2)
(3)
(4)
(5)
(6)
(7)
(8)
(9)
(10)
(11)
(12)
(13)
(14)
(15)
(16)
(17)
(18)
(19)
(20)
(21)
(22)
(23)
(24)
(25)
(26)
(27)
(28)
(29)
(30)
(31)
(32)
(33)

FIGURE 2

by the thermal history of the sample prior to being cooled to constant composition. A number of studies covering temperature ranges above 1000 K are not included, because in this region the O/Ni ratio changes with temperature, due to rapid equilibration involving the exchange of oxygen between the solid and the ambient. The measurements in this high temperature range are therefore crucially dependent on the partial pressure of oxygen in the atmosphere surrounding the sample and are not intrinsic to NiO.

Several features of Fig. 1 are noteworthy: There is an enormous spread in resistivity values; at room temperature ρ lies in the range 10^3 to 10^{13} ohm-cm for single crystals. The particular value depends, among other matters, quite sensitively on δ, which quantity is restricted to the range $0 \leq \delta \lesssim 5X10^{-3}$ in the homogeneity domain for nickel oxide. As δ decreases towards its lower limit the resistivity increases; the most nearly stoichiometric specimens become good insulators. This is so because the density of holes is controlled primarily through the density of nickel ion vacancies, which, having an effective double negative charge each, are associated with two holes that maintain electroneutrality. In a perfect crystal for which $\delta = 0$, there would be no excess charge carriers for net charge transport; in actuality, the exact 1:1 O/Ni stoichiometry cannot be realized, and the presence of impurities and other types of defects furnishes sufficient carriers for some observable conductivity. The upper limit on the resistivity which can currently be achieved with the best available samples is shown as the uppermost curve, Curve A, in Fig. 1. The lone curve (curve 4) which is shown as lying higher in resistivity was reported for a thin NiO film on MgO and appears to be spurious. For intermediate stoichiometry the recommended values are shown in Curve B. The lower limit, attained for $\delta \approx 5X10^{-3}$, is shown as Curve C in Fig. 1. It is seen that nearly all the measurements reported in the literature fall within the indicated

range; there seems no reason for questioning any of these results. Whatever differences are encountered presumably are due to differences in δ among the various samples.

The variation of resistivity with temperature is rather complex. Most noticeable are the rather marked changes of slope in the plots of Fig. 1 close to the vicinity of the Néel point at $T_N \approx 523$ K. These changes are not abrupt but occur over an interval of 40-70 degrees in the vicinity of T_N. At higher temperatures the resistivity activation energies ε_ρ range between 0.30 eV for $\delta \approx 0$ to 0.20 eV for $\delta \approx 5X10^{-3}$. For most of the data reported at lower temperatures it is not possible to specify a unique conductivity activation energy since the plots in this range of temperatures are not strictly linear. However, the average values of ε_ρ are approximately 0.80 eV for $\delta \approx 0$ and 0.66 eV for $\delta \approx 5X10^{-3}$. An interpretation for these facts is offered in Sec. 3.2 where the curves for the recommended values will also be explained.

Reasons have already been adduced why resistivity measurements carried out on polycrystalline, ceramic, sintered, pressed, or powdered specimens should be regarded with great caution. Aside from the difficulties introduced earlier, the problem which is peculiar to NiO is that untreated surface layers tend to be strongly Ni-deficient, as judged by XPS (ESCA) experiments.[24] We therefore do not recommend any of the resistivity values in Fig. 2 as being representative of bulk NiO, although these measurements are of intrinsic interest in certain industrial and engineering applications. It is to be noted that at room temperature quoted resistivities lie in the range $3X10^2$ to 10^{10} ohm-cm, i.e., considerably below the range of ρ values quoted for single crystals. Also, the conductivity activation energies tend to be lower and the changes in slope near the Néel point less than for single crystals. The limiting curves shown in Fig. 2 represent empirical boundaries within which all

TABLE 2. MEASUREMENT INFORMATION ON THE ELECTRICAL RESISTIVITY OF SINGLE CRYSTAL $Ni_{1-\delta}O$

Cur. No.	Ref. No.	Author(s)	Year	Method Used	Temp. Range, K	Name and Specimen Designation	Composition (weight percent), Specifications, and Remarks
1	28	Parravano, G.	1955	V	333-1000		No details reported.
2	29	Austin, I. G., Springthorpe, A. J., Smith, B. A. and Turner, C. E.	1967	V and A	386-613		Single crystal grown on <111> axes. Rectangular block cut. Annealed at 1400 K. Stressed on <111> axis. T_N=523 K. Measured in air.
3	30	Friedman, F., Weichman, F. L., and Tannhauser, D.	1975	P	444-780		Single crystals 1x2x(0.01 to 0.02)cm³ made by halide decomposition method. Brought to equilibrium with oxygen and argon at 1173 K. Measured in oxygen partial pressure of $3x10^{-1}$ torr.
4	31	Ksendzov, Ya.M. and Drabkin, I. A.	1965		670-1190		Made by halide decomposition method. Measured at pressure in vacuum of 10^{-4} mm Hg.
5	32	Koide S.	1965	A	620-891	L.0	Single crystal film 8 mm x 8 mm x 13μ epitaxially grown by halide decomposition method. T_N=523 K. Measured in argon.
6	33	Morin, F. J.	1954		190-1300		No details reported.
7	34	Yamaka, E. and Sawamoto, K.	1958	A			Single crystals cleaved into rectangular parallelopipeds. Manufactured by Tochigi Chemical Industrial Company, Ltd., Osaka, Japan. Grown by Verneuil method. Stress-annealed through T_C = 250° along direction <111>. Measured in air.
8	35	Vernon, M.W. and Lovell, M.C.	1966	V	291-669	A.2	Single crystal 1 mm x 1 mm x 200μ grown epitaxially by halide decomposition method. T_N=523 K. Measured in air.
9	35	Vernon, M.W. and Lovell, M.C.	1966	V	291-670	A.2	Same as above, but annealed.
10	35	Vernon, M.W. and Lovell, M.C.	1966	V	301-657	B.1	Single crystal grown by floating zone method using carbon arc image furnace. T_N=523 K. Measured in air.
11	35	Vernon, M.W. and Lovell, M.C.	1966	V	295-663	B.1	Same as above, but annealed.
12	35	Vernon, M.W. and Lovell, M.C.	1966	V	289-654	C.1	Single crystal. Small parallelopiped measuring few mm cleaved from as grown crystal. Manufactured by Fuji Titanium Co., Ltd., Japan. Grown by Verneuil technique. T_N=523 K. Measured in air.
13	35	Vernon, M.W. and Lovell, M.C.	1966	V	287-652	C.1	Same as above, but annealed.
14	36	Aiken, J.G. and Jordan, A.G.	1968	V	306-502		Single Crystal grown by halide decomposition method. Measured in dry nitrogen.
15	36	Aiken, J.G. and Jordan, A.G.	1968	V	223-500		Single crystal grown by flame fusion method. Annealed. Measured in dry nitrogen.

TABLE 2. MEASUREMENT INFORMATION ON THE ELECTRICAL RESISTIVITY OF SINGLE CRYSTAL $Ni_{1-\delta}O$ (continued)

Cur. No.	Ref. No.	Author(s)	Year	Method Used	Temp. Range, K	Name and Specimen Designation	Composition (weight percent), Specifications, and Remarks
16	36	Aiken, J.G. and Jordan, A.G.	1968	V	163-508		Single crystal grown by flame fusion method. Measured in dry nitrogen.
17	13	Osburn, C.M. and Vest, R.W.	1971	A	730-944		Single crystals manufactured by Argonne National Laboratories.
18	37	Zhuze, V.P. and Shelykh, A.I.	1963		282-695		Single crystals prepared by Verneuil method. Measured in air.
19	38	van Daal, H.J. and Bosman, A.J.	1967	A	329-1000		Single crystal 10x4x4 mm. Manufactured by Marubeni-Osaka. Measured in 1 atm of O_2.
20	39	Nowotny, J. and Wagner, J. B., Jr.	1973	A	902-986		Single crystals cleaved to 2x2x10 mm. Measured in 9.7×10^{-2} atm. of oxygen. Report temperature accurate to within ±1 K.
21	40	Melik-Davtyan, R. L., Shvartsenau, N. F., and Shelykh, A. I.	1966		684-990		Single crystals prepared by A. A. Popova of Institute of Crystallography AN SSSR. Measured in air.
22	4	Keem. J. E.	1976	V and A	333-621		Single crystals prepared by arc-transfer technique. Measured in air.
23	4	Keem. J. E.	1976	V and A	300-730		Same as above.
24	4	Keem. J. E.	1976	V and A	295-1000		Same as above.
25	4	Keem. J. E.	1976	V and A	416-704		Single crystals prepared by arc-transfer technique. Measured in air.
26	4	Keem. J. E.	1976	V and A	385-769		Same as above.
27	4	Keem. J. E.	1976	V and A	308-714		Same as above.
28	4	Keem. J. E.	1976	V and A	290-714		Same as above.
29	4	Keem. J. E.	1976	V and A	333-625		Same as above.
30	4	Keem. J. E.	1976	V and A	251-1667		Same as above.
31	4	Keem. J. E.	1976	V and A	290-800		Same as above.
32	4	Keem. J. E.	1976	V and A	290-667		Single crystals grown by arc-transfer technique. Measured in air.
33	4	Keem, J. E.	1976	V and A	177-410		Same as above.
34	4	Keem, J. E.	1976	V and A	290-758		Same as above.

TABLE 3. TABULATION OF RESISTIVITIES OF SINGLE CRYSTAL $Ni_{1-\delta}O$

[Inverse Temperature, $10^3/T$, K^{-1} : Resistivity, ρ, Ohm-cm]

$10^3/T$	ρ
CURVE 1	
1.0	1.318E+00
1.5	3.162E+00
2.0	2.454E+01
2.5	5.012E+02
3.0	1.445E+04
CURVE 2	
1.63	3.090E+01
1.66	3.311E+01*
1.70	3.630E+01
1.77	4.266E+01*
1.80	4.571E+01
1.83	5.012E+01*
1.87	5.888E+01*
1.90	7.079E+01
1.96	8.913E+01
2.02	1.230E+02
2.07	1.820E+02
2.13	2.570E+02
2.19	4.467E+02*
2.45	2.630E+03
2.53	4.900E+03
2.59	7.943E+03
CURVE 3	
1.20	6.457E+00
1.27	7.079E+00
1.32	6.761E+00
1.39	1.00 E+01
1.44	1.00 E+01
1.48	1.230E+01
1.52	1.259E+01*
1.58	1.122E+01
1.71	1.514E+01
1.82	2.570E+01
1.86	2.454E+01
1.91	3.162E+01
1.96	3.162E+01
1.96	3.981E+01
2.25	1.288E+02
CURVE 4	
0.84	4.169E+02
0.90	1.698E+03
0.96	5.129E+03

$10^3/T$	ρ
CURVE 4 (cont.)	
0.99	1.122E+04
1.03	1.905E+04
1.06	3.715E+04
1.19	5.888E+05
1.27	2.399E+06
1.39	5.370E+07
CURVE 5	
1.122	6.887E+01
1.146	8.726E+00*
1.171	1.225E+00*
1.193	1.467E+00
1.193	1.551E+00*
1.233	2.263E+00
1.271	3.047E+00*
1.271	3.419E+00
1.294	4.160E+00
1.332	3.369E+00
1.475	1.473E+01
1.610	4.957E+01
CURVE 6	
0.770	1.066E+00
0.850	1.155E+00
0.990	1.380E+00
1.130	1.393E+00
1.330	1.200E+00
1.440	2.640E+00
2.080	4.286E+01
2.390	2.952E+02
2.590	9.960E+02
3.050	2.200E+04
3.230	6.887E+04
3.350	1.828E+05
3.600	7.692E+05
3.810	2.780E+06
4.220	2.466E+07
4.920	1.028E+09
5.270	3.964E+09
CURVE 7	
1.660	2.259E+02
1.675	2.466E+02*
1.700	2.958E+02*
1.725	3.467E+02*

$10^3/T$	ρ
CURVE 7 (cont.)	
1.750	4.055E+02*
1.775	4.797E+02*
1.800	5.546E+02
1.825	6.622E+02*
1.850	7.798E+02*
1.875	9.120E+02*
1.900	1.109E+03
1.925	1.367E+03*
1.950	1.655E+03*
1.975	2.055E+03*
2.000	2.523E+03
2.025	3.040E+03*
2.050	3.647E+03*
2.075	4.425E+03*
2.100	5.407E+03
2.125	6.653E+03*
2.150	7.962E+03*
2.175	9.840E+03*
2.200	1.216E+04*
2.215	1.371E+04
CURVE 8	
3.431	3.441E+12
3.379	2.512E+12
3.339	1.935E+12
3.259	1.308E+12*
3.210	1.221E+12*
3.216	1.023E+12*
3.200	9.40[illegible]E+11
3.147	7.13[illegible]E+11*
3.122	5.580E+11*
3.073	4.535E+11*
3.014	2.906E+11
2.952	2.362E+11*
2.919	1.877E+11
2.878	1.446E+11*
2.848	1.105E+11*
2.832	9.700E+10*
2.813	9.124E+10*
2.796	8.065E+10*
2.759	6.406E+10
2.727	5.013E+10*
2.684	3.687E+10*
2.638	2.775E+10*
2.612	2.325E+10*

$10^3/T$	ρ
CURVE 8 (cont.)	
2.576	1.878E+10*
2.546	1.470E+10*
2.529	1.295E+10*
2.508	1.122E+10
2.462	9.295E+09*
2.435	6.658E+09*
2.367	3.494E+09*
2.336	2.818E+09
2.296	2.122E+09*
2.243	1.514E+09*
2.236	1.378E+09*
2.209	1.039E+09
2.190	9,259E+08*
2.176	9.675E+08*
2.166	7.825E+08*
2.148	6.309E+08*
2.123	4.433E+08*
2.102	3.631E+08
2.094	3.020E+08*
2.061	2.650E+08*
2.045	2.222E+08*
2.001	1.470E+08
1.988	1.402E+08*
1.948	1.023E+08*
1.928	7.587E+07*
1.916	6.920E+07*
1.903	5.981E+07
1.885	5.170E+07*
1.872	4.897E+07*
1.861	4.433E+07*
1.852	4.299E+07*
1.835	3.549E+07*
1.810	3.389E+07*
1.793	2.928E+07*
1.778	2.610E+07*
1.759	2.326E+07*
1.743	2.010E+07*
1.728	1.820E+07*
1.709	1.597E+07
1.691	1.402E+07*
1.668	1.240E+07*
1.656	1.175E+07*
1.646	1.080E+07*
1.621	9.479E+06*
1.602	8.130E+06
1.587	7.133E+06*
1.574	6.557E+06*

$10^3/T$	ρ
CURVE 8 (cont.)	
1.552	5.669E+06
1.520	4.399E+06*
1.506	4.013E+06*
1.495	3.891E+06
CURVE 9	
3.411	6.761E+12
3.381	5.666E+12*
3.347	3.831E+12
3.332	3.831E+12*
3.238	2.089E+12*
3.217	1.806E+12
3.192	1.370E+12*
3.170	1.088E+12*
3.148	9.124E+11*
3.112	9.124E+11
3.095	6.689E+11*
3.073	6.689E+11*
3.042	4.570E+11
2.974	2.455E+11*
2.910	1.597E+11
2.892	1.166E+11*
2.815	7.413E+10*
2.802	5.935E+10
2.754	4.331E+10*
2.714	2.531E+10
2.679	2.531E+10*
2.652	2.042E+10*
2.619	1.249E+10
2.585	9.699E+09*
2.562	7.587E+09*
2.523	5.288E+09*
2.500	4.897E+09
2.457	3.521E+09*
2.445	2.651E+09*
2.399	1.765E+09*
2.377	1.230E+09*
2.359	1.230E+09
2.322	7.764E+08*
2.302	5.935E+08*
2.266	4.466E+08*
2.256	3.715E+08
2.191	1.647E+08*
2.184	1.995E+08*
2.156	1.468E+08*
2.141	1.230E+08*

$10^3/T$	ρ
CURVE 9 (cont.)	
2.122	1.055E+08
2.095	6.406E+07*
2.073	5.128E+07*
2.048	5.128E+07*
2.010	2.952E+07
1.961	1.622E+07*
1.918	1.080E+07*
1.908	8.842E+06
1.895	6.506E+06*
1.879	5.537E+06*
1.863	4.677E+06*
1.840	4.734E+06*
1.823	3.659E+06*
1.809	2.862E+06
1.783	2.344E+06*
1.769	2.222E+06*
1.745	1.820E+06*
1.731	1.634E+06*
1.718	1.413E+06
1.696	1.175E+06*
1.684	7.194E+05*
1.660	7.413E+05*
1.642	6.863E+05*
1.623	5.580E+05*
1.607	4.606E+05
1.585	3.920E+05*
1.567	3.261E+05*
1.547	2.818E+05*
1.532	2.417E+05*
1.504	2.171E+05*
1.492	1.751E+05
CURVE 10	
3.321	3.687E+06
3.272	2.590E+06*
3.251	2.256E+06
3.224	1.905E+06*
3.210	1.585E+06
3.181	1.391E+06*
3.159	1.202E+06*
3.117	8.511E+05
3.096	7.709E+05*
3.076	6.456E+05*
3.035	4.851E+05
2.999	3.802E+05*
2.949	2.551E+05

*Not shown in figure.

TABLE 3. TABULATION OF RESISTIVITIES OF SINGLE CRYSTAL $Ni_{1-\delta}O$ (continued)

$\frac{10^3}{T}$	ρ
CURVE 10 (cont.)	
2.899	1.862E+05*
2.841	1.240E+05*
2.794	7.704E+04*
2.742	6.309E+04
2.693	4.266E+04*
2.631	2.928E+04
2.566	1.685E+04*
2.525	1.157E+04
2.462	6.974E+03*
2.427	5.089E+03
2.387	3.861E+03*
2.349	2.256E+03
2.299	1.806E+03*
2.257	1.339E+03
2.226	1.063E+03*
2.183	7.299E+02*
2.141	5.051E+02*
2.112	3.891E+02
2.078	3.030E+02*
2.051	2.418E+02*
2.022	1.950E+02*
2.003	1.647E+02
1.976	1.359E+02*
1.936	1.000E+02*
1.917	9.407E+01*
1.904	7.825E+01
1.880	7.077E+01*
1.848	5.981E+01
1.801	4.677E+01*
1.786	4.331E+01*
1.735	3.494E+01*
1.707	3.285E+01
1.669	2.650E+01*
1.642	2.326E+01
1.577	2.058E+01*
1.538	1.685E+01*
1.522	1.502E+01
CURVE 11	
3.392	1.088E+07
3.371	8.984E+06*
3.334	7.246E+06*
3.319	6.812E+06*
3.305	6.072E+06
3.260	4.824E+06*

$\frac{10^3}{T}$	ρ
CURVE 11 (cont.)	
3.251	4.011E+06
3.220	3.311E+06*
3.193	3.043E+06*
3.151	2.186E+06
3.137	1.778E+06*
3.082	1.328E+06*
3.034	1.008E+06*
3.006	8.251E+05
2.947	5.051E+05*
2.925	4.570E+05*
2.892	3.861E+05*
2.875	3.414E+05*
2.850	2.840E+05
2.816	2.154E+05*
2.751	1.711E+05*
2.704	1.562E+05*
2.704	1.088E+05
2.659	7.704E+04*
2.612	6.506E+04*
2.550	3.604E+04
2.534	2.512E+04*
2.515	2.754E+04*
2.459	1.738E+04
2.438	1.328E+04*
2.375	8.065E+03*
2.338	7.299E+03
2.281	4.713E+03*
2.275	3.494E+03*
2.261	2.630E+03*
2.245	2.344E+03*
2.226	2.042E+03
2.176	1.525E+03*
2.128	9.775E+C *
2.107	8.319E+02
2.089	7.358E+02*
2.065	5.754E+02*
2.040	4.537E+02

$\frac{10^3}{T}$	ρ
CURVE 11 (cont.)	
2.024	4.105E+02*
2.002	3.575E+02
1.973	2.610E+02*
1.955	2.222E+02
1.942	2.222E+02*
1.923	2.010E+02*
1.905	1.751E+02*
1.871	1.380E+02*
1.855	1.259E+02
1.837	1.131E+02*
1.786	1.000E+02*
1.769	1.000E+02*
1.740	7.943E+01
1.695	6.215E+01*
1.672	5.089E+01*
1.656	4.824E+01*
1.638	4.202E+01*
1.623	4.202E+01
1.594	3.390E+01*
1.563	3.211E+01*
1.545	3.067E+01*
1.527	2.733E+01*
1.509	2.473E+01
CURVE 12	
3.461	2.171E+07
3.432	1.606E+07*
3.371	1.339E+07
3.307	6.072E+06
3.231	4.787E+06*
3.177	2.650E+06*
3.121	1.905E+06
3.037	9.922E+05*
3.006	7.880E+05
2.954	5.580E+05*
2.939	4.751E+05*
2.880	3.236E+05*
2.806	1.724E+05
2.774	1.157E+05*
2.711	1.031E+05*
2.666	7.299E+04*
2.610	4.975E+04
2.595	3.289E+04*
2.550	2.797E+04*
2.525	2.571E+04*

$\frac{10^3}{T}$	ρ
CURVE 12 (cont.)	
2.501	1.965E+04
2.472	1.433E+04*
2.464	1.359E+04*
2.440	1.148E+04*
2.424	1.015E+04*
2.411	9.259E+03
2.385	7.413E+03*
2.368	6.605E+03*
2.326	4.399E+03*
2.307	3.659E+03
2.249	2.436E+03*
2.202	1.585E+03
2.184	1.370E+03*
2.173	1.148E+03*
2.146	1.000E+03*
2.122	8.643E+02*
2.105	6.812E+02
2.073	6.064E+02*
2.071	4.466E+02*
2.052	4.137E+02*
2.000	3.043E+02
1.995	2.122E+02*
1.978	2.436E+02*
1.969	1.549E+02*
1.957	2.155E+02*
1.948	2.692E+02*
1.932	1.672E+02*
1.909	1.318E+02*
1.891	1.212E+02*
1.872	9.775E+01
1.855	9.328E+01*
1.846	7.825E+01*
1.835	7.704E+01*
1.811	6.456E+01*
1.799	5.797E+01*
1.783	5.453E+01*
1.769	4.935E+01*
1.755	4.167E+01
1.737	4.167E+01*
1.720	3.802E+01*
1.701	3.163E+01*
1.660	3.163E+01*
1.646	2.754E+01*
1.631	2.205E+01*
1.600	2.058E+01
1.575	1.820E+01*

$\frac{10^3}{T}$	ρ
CURVE 12 (cont.)	
1.543	1.672E+01*
1.530	1.514E+01*
CURVE 13	
3.481	3.138E+08
3.475	4.433E+08*
3.370	2.058E+08*
3.347	1.968E+08
3.296	1.278E+08*
3.288	8.985E+07*
3.228	6.215E+07
3.182	4.367E+07*
3.157	4.787E+07*
3.114	2.754E+07
3.087	3.211E+07*
3.073	1.995E+07*
3.007	1.778E+07
2.991	1.278E+07*
2.960	9.921E+06*
2.934	1.157E+06*
2.913	8.71 E+06*
2.860	4.502E+06
2.791	4.502E+06*
2.788	2.650E+06*
2.742	3.415E+06*
2.742	2.326E+06*
2.703	1.698E+06
2.674	1.891E+06*
2.625	1.328E+06
2.596	8.711E+05*
2.575	7.138E+05*
2.527	4.011E+05*
2.504	4.011E+05
2.497	5.411E+05*
2.435	2.273E+05*
2.412	2.273E+05*
2.394	1.642E+05*
2.374	1.659E+05*
2.359	1.193E+05
2.326	8.913E+04*
2.275	5.981E+04*
2.256	4.606E+04*
2.204	2.915E+04
2.149	1.871E+04*
2.132	1.537E+04

$\frac{10^3}{T}$	ρ
CURVE 13 (cont.)	
2.099	1.288E+04*
2.080	1.113E+04*
2.039	6.897E+03*
2.000	4.762E+03
1.975	4.739E+03*
1.968	3.52 E+03*
1.916	2.473E+03*
1.901	1.965E+03
1.875	1.537E+03*
1.854	1.063E+03*
1.827	8.065E+02*
1.806	6.812E+02
1.793	6.557E+02*
1.774	4.936E+02*
1.754	3.920E+02*
1.723	3.715E+02
1.696	2.797E+02*
1.649	2.010E+02*
1.638	1.848E+02*
1.612	1.711E+02
1.586	1.359E+02*
1.578	1.202E+02*
1.548	1.080E+02*
1.535	8.913E+01
CURVE 14	
1.990	3.191E+07
2.030	5.811E+07*
2.090	9.597E+07*
2.120	1.629E+08
2.190	3.389E+08*
2.250	5.624E+08
2.230	1.052E+09*
2.370	2.023E+09
2.440	3.206E+09
2.510	5.727E+09
2.590	1.236E+10*
2.640	2.023E+10*
2.690	3.357E+10
2.810	5.970E+10*
2.910	1.276E+11
2.960	3.206E+11*
3.060	6.821E+11
3.140	1.413E+12*
3.270	3.673E+12

*Not shown in figure.

TABLE 3. TABULATION OF RESISTIVITIES OF SINGLE CRYSTAL $Ni_{1-x}O$ (continued)

$\frac{10^3}{T}$	ρ
CURVE 15	
2.000	1.005E+04
2.070	1.954E+04*
2.150	3.373E+04
2.190	6.698E+04*
2.250	1.000E+05
2.310	1.762E+05
2.380	3.034E+05*
2.440	5.322E+05
2.520	1.028E+06
2.600	1.738E+06
2.640	3.236E+06*
2.730	5.917E+06
2.790	1.208E+07*
2.870	2.366E+07
2.970	5.999E+07
3.110	1.563E+08
3.220	4.808E+08
3.300	1.009E+09
3.390	2.168E+09
3.470	4.529E+09
3.580	1.208E+10
3.700	3.580E+10
3.770	5.249E+10*
3.830	9.251E+10
3.890	1.607E+11*
3.970	2.547E+11
4.020	3.597E+11
4.090	5.624E+11
4.120	8.354E+11*
4.190	1.236E+12
4.260	1.871E+12
4.360	3.664E+12
4.490	7.587E+12
CURVE 16	
1.970	3.281E+02
2.060	6.337E+02
2.130	9.251E+02
2.200	1.361E+03
2.260	2.168E+03*
2.310	3.076E+03
2.440	6.541E+03
2.480	9.506E+03
2.530	1.439E+04
2.600	2.168E+04
2.670	3.873E+04

$\frac{10^3}{T}$	ρ
CURVE 16 (cont.)	
2.740	6.821E+04
2.910	1.730E+05
3.010	3.133E+05
3.080	6.223E+05*
3.180	9.996E+05
3.280	1.986E+06
3.370	3.467E+06
3.450	6.053E+06
3.540	9.293E+06
3.630	1.941E+07
3.750	3.945E+07
3.860	7.981E+07
3.960	1.722E+08
4.090	3.733E+08
4.200	7.837E+08
4.330	2.070E+09
4.470	4.897E+09
4.560	8.319E+09
4.710	1.778E+10
4.780	2.938E+10*
4.920	5.013E+10
4.980	6.309E+10*
5.070	1.087E+11
5.170	1.941E+11
5.370	3.435E+11
5.480	5.470E+11
5.570	8.091E+11
5.660	1.112E+11
5.750	1.578E+12
5.830	1.714E+12
5.950	2.871E+12
6.070	3.766E+12
6.150	3.766E+12
CURVE 17	
1.062	5.610E+00
1.159	4.602E+00
1.259	5.967E+00
1.377	6.668E+00
CURVE 18	
1.44	7.413E+00
1.64	1.778E+01
1.80	3.467E+01
1.90	5.248E+01

$\frac{10^3}{T}$	ρ
CURVE 18 (cont.)	
2.20	1.778E+02
2.36	4.365E+02
2.55	1.259E+03
2.74	3.236E+03
2.74	4.365E+03
2.94	1.445E+04
3.05	2.692E+04
3.15	4.677E+04
3.18	7.762E+04
3.22	9.120E+04
3.43	2.754E+05
3.53	5.129E+05
3.54	3.890E+05
CURVE 19	
1.00	3.090E+00
1.10	3.981E+00
1.20	4.365E+00
1.30	5.495E+00
1.40	7.413E+00
1.50	1.00 E+01
1.60	1.698E+01
1.70	2.951E+01
1.80	4.786E+01*
1.90	8.128E+01*
2.00	1.380E+02
2.10	2.512E+02
2.20	5.012E+02
2.30	9.550E+02
2.40	1.995E+03
2.50	4.266E+03
2.60	9.333E+03
2.70	1.950E+04
2.80	4.571E+04
2.90	9.772E+04
3.00	2.291E+05
3.04	3.311E+05
CURVE 20	
1.014	2.400E+02
1.037	2.754E+02
1.062	3.090E+02
1.083	3.467E+02
1.107	4.074E+02

$\frac{10^3}{T}$	ρ
CURVE 21	
1.462	-1.023E+01
1.361	8.710E+00
1.307	6.918E+00
1.258	5.754E+00*
1.126	4.677E+00
1.082	3.630E+00
1.010	1.905E+00
CURVE 22	
1.61	1.002E+07
1.73	1.995E+07
1.86	3.447E+07
1.99	7.079E+07
2.13	2.304E+08
2.19	5.463E+08
2.27	9.716E+08
2.36	1.996E+09
2.43	4.870E+09
2.51	1.059E+10
2.58	2.304E+10
2.78	8.660E+10
3.00	2.818E+11
CURVE 23	
1.37	2.113E+02
1.61	3.981E+02
1.77	8.410E+02
1.97	2.900E+03
2.14	1.330E+04
2.33	6.130E+04
2.42	1.413E+05
2.55	2.738E+05
2.78	1.585E+06
2.99	1.189E+07
3.33	4.730E+07
CURVE 24	
1.00	1.000E+02
1.30	2.238E+02
1.50	3.981E+02
1.60	5.158E+02
1.81	9.716E+02
1.99	3.981E+03
2.18	1.454E+04

$\frac{10^3}{T}$	ρ
CURVE 24 (cont.)	
2.38	6.685E+04
2.42	1.454E+05*
2.60	3.350E+05
2.80	1.334E+06
3.00	4.097E+06
3.38	4.597E+07
CURVE 25	
1.42	3.073E+00
1.60	4.873E+00
1.80	7.943E+00
1.91	1.000E+00
2.00	1.679E+01
2.20	5.957E+01
2.40	1.995E+02
CURVE 26	
1.3	1.090E+01
1.6	2.054E+01*
1.8	4.467E+01
2.0	1.372E+02*
2.2	5.623E+02
2.4	2.585E+03
2.6	1.00 E+04
CURVE 27	
1.40	2.661E+01
1.86	9.441E+01
2.20	1.631E+03
2.50	1.939E+04*
2.80	1.679E+05
3.25	1.939E+06
CURVE 28	
1.40	2.175E+01
1.86	7.943E+01
2.00	3.162E+02
2.20	1.259E+03
2.50	1.454E+04
2.80	1.372E+05
2.99	4.097E+05
3.45	4.870E+06

$\frac{10^3}{T}$	ρ
CURVE 29	
1.60	1.000E+01
1.81	1.778E+01
2.00	4.870E+01
2.20	1.454E+02
2.45	5.623E+02
2.60	2.441E+03
2.80	1.122E+04
3.00	4.340E+04
CURVE 30	
0.60	6.750E+00
0.56	1.155E+01
0.72	1.884E+01
0.81	2.304E+01
0.91	3.447E+01
1.01	4.730E+01
1.11	5.960E+01
1.21	7.079E+01
1.50	2.054E+02
1.69	2.585E+02
1.75	3.548E+02
1.80	3.981E+02
1.90	5.951E+02
2.00	8.175E+02
2.17	7.286E+03
2.72	2.238E+05
3.5	5.623E+06
3.99	7.943E+07
CURVE 31	
3.45	7.940E+05
3.24	4.597E+05
3.00	6.310E+04
2.85	5.010E+04
2.70	1.728E+04
2.52	3.073E+03
2.32	8.414E+02
2.20	3.447E+02
2.07	1.000E+02
1.95	3.980E+01
1.75	1.939E+01
1.50	9.173E+00
1.25	5.012E+00
0.60	1.000E+00

*Not shown in figure.

TABLE 3. TABULATION OF RESISTIVITIES OF SINGLE CRYSTAL $Ni_{1-\delta}O$ (continued)

$\frac{10^3}{T}$	ρ
CURVE 32	
1.50	1.330E+01
1.75	2.510E+01
2.00	6.490E+01
2.15	3.760E+02
2.40	1.260E+03
2.54	3.548E+03
3.00	1.540E+04
3.45	6.310E+04
CURVE 33	
2.44	8.913E+05
2.59	2.180E+06
2.79	1.060E+07
2.99	4.100E+07
3.19	1.630E+08
3.40	2.512E+08
3.58	2.239E+09
3.78	7.286E+09
3.98	2.110E+10
4.17	5.16 E+10
4.37	1.223E+11
4.52	3.447E+11
4.62	1.092E+12
4.77	1.884E+12
4.97	5.620E+12
5.28	1.995E+13
5.42	4.597E+13
5.66	1.000E+14
CURVE 34	
1.32	6.131E+01
1.50	9.173E+01
1.70	1.679E+02
1.80	2.113E+02
2.00	5.463E+02
2.20	3.255E+03
2.40	1.585E+04
2.60	6.683E+04
2.84	3.162E+05
3.00	1.223E+06
3.28	4.097E+06
3.45	1.000E+07

TABLE 4. MEASUREMENT INFORMATION ON THE ELECTRICAL RESISTIVITY OF POLYCRYSTAL $Ni_{1-\delta}O$

Cur. No.	Ref. No.	Author(s)	Year	Method Used	Temp. Range, K	Name and Specimen Designation	Composition (weight percent), Specifications, and Remarks
1	28	Parravano, G.	1955	V	380-901		Sample prepared by thermal decomposition of solutions of cp nitrates, ground, and fired in air for 4 h at 1173 K. Contacts were platinum foil. Measured in air.
2	33	Morin, F. J.	1954		83-1220		Sample obtained by thermal decomposition of $Ni(NO_3)_2$ at 1473 K for 16 h in O_2.
3	33	Morin, F. J.	1954		87-813		Sample obtained by thermal decomposition of $Ni(NO_3)_2$ at 1773 K for 2 h in air.
4	13	Osburn, C. M. and Vest, R. W.	1971	A	728-943		Samples obtained from Argonne National Laboratories.
5	37	Zhuze, V. P. and Shelykh, A. I.	1963		495-775		Alkaline $NiCO_3$ fired, compacted at 9000 Kg/cm^2, annealed in air for 6 h at 1473 K. Density 80-85% of x-ray density. Measured in air.
6	41	van Houten, S.	1960	A	315-775		Bars or discs. $NiCO_3$ fired at 900°C, milled, and hydrostatically pressed at 10 tons/cm^2. Fired in air at 1823 K. Cooled from 1073 K in N_2. Density 88-95% of maximum. Contacts were graphite or In-Hg amalgam. Measured in air.
7	41	van Houten, S.	1960	A	303-725		Specimen from the same batch as the above specimen. Same procedure.
8	41	van Houten, S.	1960	A	313-935		Specimen from the same batch as the above specimen. Same procedure.
9	41	van Houten, S.	1960	A	383-769		Specimen from the same batch as the above specimen. Same procedure.
10	42	Nachman, M., Cojocaru, L. N., and Rîbco, L. V.	1965	A	301-719	A	Cylindrical sample. Thermal decomposition of $NiCO_3$ at 873 K. Pressed at 1.5 t/cm^2. Heated in air for 20 h at decomposition temperature. Density 76.5% of maximum. T_N=523 K. Contacts were Pt. Measured in air.
11	42	Nachman, M., Cojocaru, L. N., and Rîbco, L. V.	1965	A	300-794	B	Same as above except decomposition temperature was 973 K.
12	42	Nachman, M., Cojocaru, L. N., and Rîbco, L. V.	1965	A	296-826	C	Same as above except decomposition temperature was 1073 K and density 81.0% of maximum.
13	42	Nachman, M., Cojocaru, L. N., and Rîbco, L. V.	1965	A	298-820	D	Same as above except decomposition temperature was 1173 K and density 84.0% of maximum.
14	42	Nachman, M., Cojocaru, L. N., and Rîbco, L. V.	1965	A	297-893	E	Same as above except decomposition temperature was 1273 K and density 87.0% of maximum.
15	25	Notis, M. R., Spriggs, R. M., and Hahn, W. C., Jr.	1973	A	294-752		Rectangular bars. 99.999% pure NiO powder from Johnson-Matthey Co. Air fired at 1173 K for 10 h, ground, dried for 24 h at 413 K. Pressure-sintered at 10 000 psi and 1373 K for 90 min. Density 92.0-99.93% of x-ray density. T_N=523 K. Contacts were Pt. Measured in air.

TABLE 4. MEASUREMENT INFORMATION ON THE ELECTRICAL RESISTIVITY OF POLYCRYSTAL $Ni_{1-\delta}O$ (continued)

Cur. No.	Ref. No.	Author(s)	Year	Method Used	Temp. Range, K	Name and Specimen Designation	Composition (weight percent), Specifications, and Remarks
16	43	Shimomura, Y. and Tsubokawa, I.	1954		375-573		3.5 mm diameter and 6 mm length.
17	44	Cimino, A., Molinari, E., and Romeo, G.	1958	V	345-654		Thermal decomposition of nickel nitrate at 573 K. Heat treatment 3 h in air at 913 K. Measured in air at slowly rising temperature.
18	44	Cimino, A., Molinari, E., and Romeo, G.	1958	V	335-654		Same as above, but measured at slowly decreasing temperature.
19	45	Wright, R. W. and Andrews, J. P.	1949	V	443-662	A_1	Nickel foil oxidized at 1273 K for 30 h. Contacts silver. Measured in air.
20	45	Wright, R. W. and Andrews, J. P.	1949	V	437-771	A_2	Sample from same batch as the above. Same procedure.
21	45	Wright, R.W. and Andrews, J. P.	1949	V	420-779	B_1	Sample from same batch as the above. Same procedure.
22	45	Wright, R. W. and Andrews, J. P.	1949	V	408-788	B_2	Sample from same batch as the above. Same procedure.
23	45	Wright, R. W. and Andrews, J. P.	1949	V	458-726	E	Sample from same batch as the above. Same procedure.
24	45	Wright, R. W. and Andrews, J. P.	1949	V	516-758	G	Sample from same batch as the above. Same procedure
25	40	Melik-Davtyan, R. L., Shvartsenau, N. F., and Shelykh, A. I.	1966		760-1006		Nickel nitrate dried at 393-423 K, roasted at 1573 K for 2 h and converted into NiO. Measured in air.
26	46	Foëx, M.	1952	V	347-680	A	Rods 10 mm long, 7 mm diameter; thermal decomposition at 773 K of $Ni(NO_3)_2$; pressed NiO powder; platinum electrodes.
27	46	Foëx, M.	1952	V	347-735	B	Same as above except decomposed at 873 K.
28	46	Foëx, M.	1952	V	347-980	C	Same as above except decomposed at 1073 K.
29	46	Foëx, M	1952	V	347-980	D	Same as above except decomposed at 1373 K.
30	46	Foëx, M.	1952	V	347-980	E	Same as above except decomposed at 1673 K.
31	46	Foëx, M.	1952	V	398-980	F	Same as above except decomposed at about 2273 K, or near the melting point of NiO.
32	47	von Baumbach, H. H. and Wagner, C.	1933	V	620-871	Probe 2	Nickel strips 0.05 to 0.07 mm thick oxidized for 1 to 2 days at 1273 K in air.

TABLE 4. MEASUREMENT INFORMATION ON THE ELECTRICAL RESISTIVITY OF POLYCRYSTAL $Ni_{1-\delta}O$ (continued)

Cur. No.	Ref. No.	Author(s)	Year	Method Used	Temp. Range, K	Name and Specimen Designation	Composition (weight percent), Specification, and Remarks
33	47	von Baumbach, H. H. and Wagner, C.	1933	V	653-889	Probe 3	Same as above.
34	48	Schlosser, E. G.	1961	V	323-873		Thermal decomposition of $NiCO_3$ for 5 h at 1273 K, washed in H_2O then heated again to 1273 K for 5 h; pressed NiO powder; silver paste electrodes.

TABLE 5. TABULATION OF RESISTIVITIES OF POLYCRYSTAL $Ni_{1-\delta}O$

[Inverse Temperature, $10^3/T$, K^{-1}; Resistivity, ρ, Ohm cm]

$\frac{10^3}{T}$	ρ
CURVE 1	
1.11	6.310E+01
1.22	7.943E+01
1.57	5.012E+02
1.75	7.943E+02
2.27	1.000E+04
2.63	5.129E+04
CURVE 2	
0.820	3.420E+00
0.890	3.499E+00
1.000	3.926E+00
1.250	4.764E+00
1.590	9.775E+00
1.870	3.837E+01
2.050	1.241E+02
2.190	3.034E+02
2.550	2.489E+03
2.860	1.000E+04
3.320	6.337E+04
4.430	3.908E+06
5.070	2.655E+07
5.500	6.196E+07
6.580	3.076E+08
8.160	7.179E+08*
8.910	7.446E+08*
12.000	7.446E+08*
CURVE 3	
1.230	3.766E+00
1.330	4.100E+00
1.450	4.509E+00
1.840	8.130E+00
1.940	1.000E+01
2.030	1.374E+01
2.180	2.334E+01
2.240	2.754E+01
2.370	4.897E+01
2.660	2.004E+02
2.920	6.024E+02
3.330	2.884E+03
3.570	6.854E+03
3.900	1.698E+04
4.470	8.554E+04
4.920	2.793E+05
CURVE 3 (cont.)	
5.410	9.001E+05
5.750	7.803E+06
6.170	3.873E+06
6.860	1.459E+07
7.500	5.035E+07
8.210	2.061E+08*
9.670	1.175E+09*
11.500	6.398E+09*
CURVE 4	
1.000	5.943E+00
1.159	6.124E+00
1.256	6.310E+00
1.375	6.668E+00
CURVE 5	
1.29	6.166E+00
1.32	7.244E+00*
1.42	1.096E+01
1.43	1.349E+01*
1.47	1.659E+01*
1.46	1.995E+01*
1.51	2.291E+01
1.60	4.109E+01
1.72	1.00 E+02
1.74	1.380E+02*
1.82	3.020E+02
1.88	4.266E+02*
1.89	6.166E+02*
2.02	2.344E+03
CURVE 6	
1.29	9.759E+02
1.43	2.849E+03
1.46	4.127E+03
1.63	3.530E+04
1.97	3.851E+05
2.04	6.924E+05
2.11	1.399E+06
2.31	5.450E+06
2.36	6.872E+06
2.60	2.372E+07
2.75	5.137E+07
CURVE 6 (cont.)	
2.76	6.013E+07*
2.98	1.306E+08
3.20	5.557E+08
CURVE 7	
1.38	6.168E+03
1.53	2.428E+04
1.77	2.148E+05
1.79	3.955E+05
1.85	5.792E+05
1.95	2.089E+06
2.05	4.499E+06
2.19	1.022E+07
2.37	1.974E+07
2.68	1.520E+08
2.81	2.893E+08
2.96	4.997E+08
3.09	1.288E+09
3.20	2.162E+09
3.30	3.173E+09
CURVE 8	
1.07	2.695E+03
1.20	7.258E+0[illegible]
1.29	1.776E+04
1.53	2.775E+05
1.64	4.625E+05
1.81	2.833E+06
2.17	6.075E+07
2.79	3.167E+09
3.05	7.389E+09
3.20	3.757E+10
CURVE 9	
1.30	1.888E+05
1.49	1.477E+06
1.60	4.852E+06
1.79	2.173E+07
2.08	1.153E+08
2.26	3.357E+08
2.61	2.106E+09
CURVE 10	
3.34	1.202E+03
3.12	7.079E+02
2.96	4.169E+02
2.63	1.445E+02
2.09	3.162E+01
1.77	9.333E+00
1.52	5.248E+00
1.39	3.236E+00
CURVE 11	
3.33	2.951E+03
3.06	1.950E+03
2.92	4.898E+02
2.50	2.188E+02
2.34	1.288E+02
2.08	5.128E+01
1.93	3.236E+01
1.84	1.862E+01
1.67	1.096E+01
1.55	7.586E+00
1.50	6.457E+00
1.44	5.495E+00*
1.37	4.575E+00
1.31	3.631E+00*
1.26	3.236E+00
CURVE 12	
3.38	2.512E+04
3.11	4.365E+03
2.80	1.202E+03
2.61	5.754E+02
2.43	2.951E+02
2.19	8.912E+01
2.06	5.888E+01
1.96	4.467E+01
1.81	2.188E+01
1.64	1.148E+01
1.42	6.166E+00
1.32	5.129E+00
1.27	4.571E+00*
1.21	4.266E+00
CURVE 13	
3.36	1.000E+05
3.10	1.862E+04
2.83	4.467E+03
2.47	4.467E+02
2.30	1.905E+02
2.18	1.259E+02
2.05	7.762E+01
1.95	5.754E+01
1.76	2.089E+01
1.71	1.698E+01
1.63	1.412E+01
1.49	1.000E+01
1.36	8.318E+00
1.25	6.166E+00*
1.22	5.754E+00
CURVE 14	
3.37	1.479E+05
3.13	2.570E+04
2.94	1.096E+04
2.59	2.455E+03
2.16	1.820E+02
1.97	6.166E+01
1.76	2.570E+01
1.65	1.738E+01
1.48	8.128E+00
1.33	6.210E+00
1.12	5.012E+00
CURVE 15	
1.33	9.912E+01
1.37	1.268E+02
1.42	1.252E+02*
1.49	1.435E+02
1.53	1.642E+02
1.60	1.931E+02
1.70	1.948E+02
1.73	2.410E+02
1.86	3.635E+02*
1.89	3.833E+02*
1.92	4.433E+02
1.97	5.439E+02*
2.02	6.377E+02
2.23	1.386E+03
CURVE 15 (cont.)	
2.37	2.987E+03
2.55	8.384E+03
2.70	1.580E+04
3.38	4.376E+04
CURVE 16	
2.674	1.608E+07
2.638	1.552E+07
2.577	1.334E+07
2.545	1.168E+07
2.500	1.024E+07
2.439	8.42 E+06
2.415	7.14 E+06
2.375	5.77 E+06*
2.375	5.54 E+06
2.347	4.72 E+06
2.309	4.19 E+06
2.272	3.17 E+06
2.237	2.81 E+06
2.127	2.40 E+06
2.188	1.88 E+06*
2.160	1.69 E+06
2.110	1.50 E+06
2.079	1.35 E+06*
2.037	1.27 E+06
2.016	1.02 E+06
1 984	0.94 E+06*
1.976	0.94 E+06
1.942	1.23 E+06
1.938	1.34 E+06*
1.908	1.32 E+06
1.923	2.22 E+06
1.862	2.57 E+06
1.845	2.75 E+06*
1.828	2.84 E+06
1.812	2.97 E+06*
1.802	2.97 E+06
1.776	2.63 E+06*
1.751	2.39 E+06*
1.742	2.29 E+06

*Not shown in figure

TABLE 5. TABULATION OF RESISTIVITIES OF POLYCRYSTAL $Ni_{1-\delta}O$ (continued)

$\frac{10^3}{T}$	ρ
CURVE 17	
1.53	1.259E+02
1.56	1.479E+02*
1.62	1.905E+02
1.67	2.511E+02
1.77	3.802E+02
1.82	5.129E+02
1.86	6.026E+02
1.89	7.244E+02*
1.92	8.709E+02
1.95	1.000E+03
1.99	1.148E+03*
2.02	1.288E+03
2.11	1.698E+03
2.22	2.570E+03
2.35	4.786E+03
2.63	1.950E+04
2.74	3.020E+04
2.90	6.457E+04
CURVE 18	
1.53	1.230E+02*
1.61	1.778E+02
1.63	1.950E+02*
1.73	3.090E+02
1.82	4.677E+02
1.86	5.623E+02*
1.92	7.762E+02
1.98	1.047E+03*
2.02	1.413E+03
2.06	1.698E+03*
2.10	2.138E+03
2.15	2.455E+03*
2.21	3.020E+03
2.24	3.388E+03*
2.31	3.890E+03
2.43	5.623E+03
2.53	8.710E+03
2.55	1.000E+04
2.60	1.175E+04
2.67	1.820E+04*
2.71	2.042E+04
2.98	7.943E+04
CURVE 19	
1.510	1.148E+04

$\frac{10^3}{T}$	ρ
CURVE 19 (cont.)	
1.640	6.026E+04
1.678	9.333E+04
1.713	1.380E+05
1.789	2.570E+05
1.852	4.786E+05
1.939	6.026E+05
2.069	1.148E+06
2.176	1.585E+06*
2.205	1.698E+06
2.258	2.188E+06
CURVE 20	
1.297	1.820E+03
1.334	3.020E+03
1.355	3.715E+03
1.439	1.096E+04
1.513	2.570E+04
1.560	4.571E+04
1.631	8.710E+04
1.694	1.380E+05
1.756	2.188E+05
1.831	3.377E+05
1.919	5.129E+05
1.999	6.918E+05
2.076	9.550E+05
2.145	1.349E+06*
2.215	1.545E+06
2.286	1.995E+06
CURVE 21	
1.283	8.913E+02
1.384	3.162E+03
1.467	8.913E+03
1.575	2.239E+04
1.608	3.631E+04*
1.694	8.913E+04*
1.744	1.175E+05
1.807	1.380E+05
1.887	1.995E+05
1.957	2.630E+05
2.055	3.467E+05
2.175	5.623E+05
2.375	8.913E+05

$\frac{10^3}{T}$	ρ
CURVE 22	
1.296	1.445E+03
1.376	3.631E+03
1.456	9.333E+03
1.558	2.889E+04
1.848	2.818E+05
1.994	5.370E+05
2.019	5.888E+05
2.147	9.333E+05
2.235	1.259E+06
2.298	1.585E+06
2.347	1.718E+06
2.452	2.512E+06
CURVE 23	
1.378	2.089E+03
1.398	2.512E+03*
1.406	2.884E+03
1.420	3.236E+03*
1.460	4.898E+03
1.526	9.772E+03
1.537	1.122E+04*
1.603	1.950E+04
1.666	2.884E+04*
1.759	4.365E+04
1.860	7.762E+04
1.969	9.772E+04
2.095	1.820E+05
2.110	1.549E+05
2.182	2.089E+05
CURVE 24	
1.320	9.120E+02
1.345	1.202E+03*
1.352	1.259E+03
1.408	2.349E+03
1.453	3.548E+03
1.507	3.370E+03
1.581	7.413E+03
1.633	9.333E+03
1.765	1.230E+04
1.808	1.318E+04
1.890	1.350E+04
1.894	1.549E+04
1.939	1.820E+04

$\frac{10^3}{T}$	ρ
CURVE 25	
1.316	1.349E+01
1.099	1.148E+01
0.994	1.175E+01
CURVE 26	
2.88	1.445E+04
2.68	6.456E+03
2.51	3.236E+03
2.36	1.738E+03
2.23	1.00 E+03
2.11	6.026E+02
2.00	3.981E+02
1.95	3.311E+02
1.90	2.092E+02
1.86	2.344E+02
1.82	1.950E+02
1.74	1.413E+02
1.66	1.096E+02
1.59	8.511E+01
1.47	5.623E+01
CURVE 27	
2.88	2.40 E+04
2.68	1.00 E+04
2.51	4.786E+03
2.36	2.455E+03
2.23	1.349E+03*
2.11	7.762E+02
2.00	5.012E+02
1.95	4.169E+02
1.90	3.468E+02
1.86	2.884E+02*
1.82	2.512E+02
1.74	1.995E+02
1.66	1.585E+02
1.59	1.318E+02
1.47	9.550E+01
1.36	7.244E+01
CURVE 28	
2.88	5.888E+04
2.68	2.138E+04*
2.51	9.120E+03
2.36	4.266E+03

$\frac{10^3}{T}$	ρ
CURVE 28 (cont.)	
2.23	2.138E+03
2.11	1.148E+03
2.00	6.607E+02
1.95	5.370E+02
1.90	4.365E+02*
1.86	3.631E+02*
1.82	3.162E+02*
1.74	2.512E+02*
1.66	1.995E+02*
1.59	1.738E+02
1.47	1.259E+02
1.36	1.000E+02
1.27	7.586E+01
1.13	5.129E+01
1.02	3.715E+01
CURVE 29	
2.88	1.259E+05
2.68	4.266E+04
2.51	1.738E+04
2.36	7.586E+03
2.23	3.715E+03
2.11	1.950E+03
2.00	1.096E+03
1.95	8.511E+02
1.90	6.607E+02*
1.86	5.623E+02
1.82	4.898E+02*
1.74	3.802E+02
1.66	2.951E+02
1.59	2.511E+02
1.47	1.862E+02
1.36	1.445E+02
1.27	1.122E+02
1.13	7.586E+01
1.02	5.495E+01
CURVE 30	
2.88	6.918E+05
2.68	2.138E+05
2.51	7.244E+04
2.36	2.818E+04
2.23	1.259E+04
2.11	6.310E+03
2.00	3.090E+03

$\frac{10^3}{T}$	ρ
CURVE 30 (cont.)	
1.95	2.344E+03
1.90	1.738E+03
1.86	1.380E+03
1.82	1.175E+03
1.74	8.071E+02
1.66	6.607E+02
1.59	5.370E+02
1.47	3.802E+02
1.36	2.692E+02
1.27	2.042E+02
1.13	1.318E+02
1.02	9.333E+01
CURVE 31	
2.51	1.023E+06
2.36	3.020E+05
2.23	1.072E+05
2.11	3.981E+04
2.00	2.698E+04
1.95	1.148E+04
1.90	7.762E+03
1.86	6.766E+03*
1.82	5.129E+03
1.74	3.311E+03
1.66	2.519E+03
1.59	1.905E+03
1.47	1.175E+03
1.36	7.943E+02
1.27	5.370E+02
1.13	2.951E+02
1.02	1.820E+02
CURVE 32	
1.148	1.230E+02
1.216	3.890E+02
1.345	1.950E+03
1.480	1.202E+04
1.60	6.310E+04

*Not shown in figure

TABLE 5. TABULATION OF RESISTIVITIES OF POLYCRYSTAL $Ni_{1-\delta}O$ (continued)

$\frac{10^3}{T}$	ρ
CURVE 33	
1.125	4.365E+02
1.175	6.918E+02
1.276	2.138E+03
1.328	3.981E+03
1.427	1.072E+04*
1.528	3.162E+04
CURVE 34	
3.096	2.857E+04*
2.681	3.389E+03*
2.364	7.163E+02*
2.114	2.661E+02*
1.745	6.605E+01*
1.486	3.935E+01*
1.294	2.511E+01*
1.145	2.213E+01*

*Not shown in figure

data so far reported are encountered. No recommended curve is offered for polycrystalline materials.

Measurement information is provided in Table 2 for resistivity measurements on single crystal NiO; the actual experimental results are collected in Table 3. Similar information for polycrystal NiO is displayed in Table 4, and the experimental data are tabulated in Table 5.

3.2 Seebeck Coefficient

Recommended values for the Seebeck coefficient of undoped single crystals of $Ni_{1-\delta}O$ in the range of its kinetic stability are shown in Table 6. The construction of these values is discussed below.

Seebeck coefficient measurements on single crystal specimens are rather few in number; available data are summarized in Fig. 3 as plots of α(mV/deg) vs. $10^3/T(K^{-1})$. As expected for insulators, α values are large, falling in the range 0.4 to 2.0 mV/deg. Above room temperature the data are relatively concordant, in that in almost all cases α increases as T is diminished; however, while some measurements show a change in the slope of α vs. 1/T as magnetic order sets in, no magnetic ordering effects are detectable in other sets of measurements. At room temperatures, the data diverge; in curves 1 and 2, α passes through a maximum and then decreases on cooling; whereas the remaining plots in Fig. 3 are continuing straight lines. We believe that below approximately 350 to 400 K sample resistivities of single crystals are so large that special precautions must be taken with regard to sample isolation and data acquisition to avoid serious error. Furthermore, internal strains can lead to divergencies from straight line behavior in Fig. 3. Accordingly, our recommended values left the low temperature variations of curves 1 and 2 out of account.

TABLE 6

RECOMMENDED VALUES FOR THE SEEBECK COEFFICIENTS OF SINGLE CRYSTAL $Ni_{1-\delta}O$ IN THE RANGE OF ITS KINETIC STABILITY

Temperature, K	SEEBECK COEFFICIENT, mV/K	
	Annealed Sample A	Unannealed Sample B
1330	0.576	—
1000	0.671	—
800	0.768	—
670	0.864	0.547
570	0.960	0.609
500	1.056	0.671
440	1.152	0.733
400	1.248	0.797
360	1.346	0.859
330	—	0.920
310	—	0.982
290	—	1.044

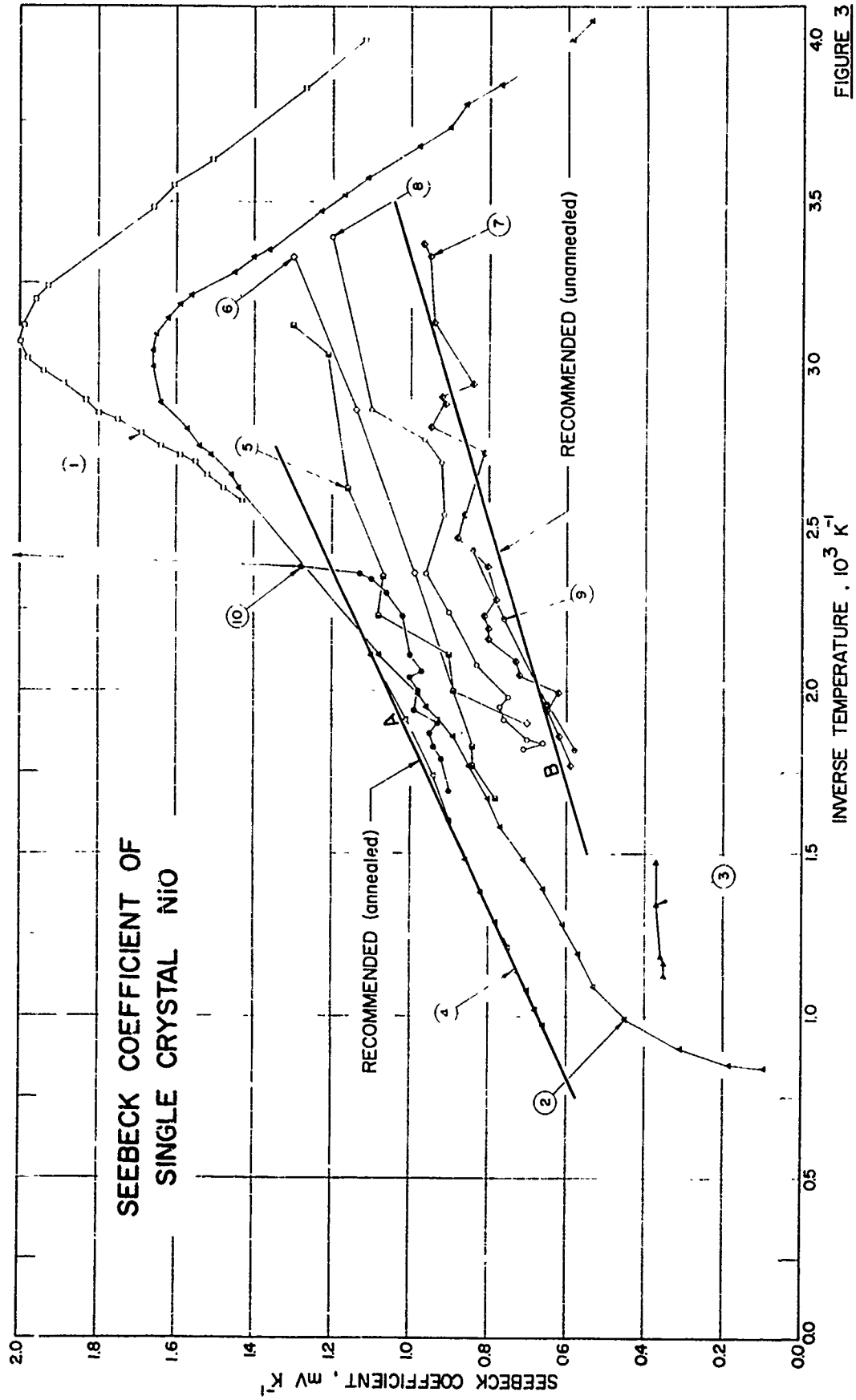
SEEBECK COEFFICIENT OF
SINGLE CRYSTAL NiO
RECOMMENDED (annealed)
RECOMMENDED (unannealed)
A
B
(1)
(2)
(3)
(4)
(5)
(6)
(7)
(8)
(9)
(10)
SEEBECK COEFFICIENT , mV K⁻¹
INVERSE TEMPERATURE , 10³ K⁻¹
0.0
0.2
0.4
0.6
0.8
1.0
1.2
1.4
1.6
1.8
2.0
0.0
0.5
1.0
1.5
2.0
2.5
3.0
3.5
4.0

FIGURE 3

The simplest interpretation of the data in Figs. 1 and 3 is to assume that charge carrier transport in $Ni_{1-\delta}O$ occurs by a hopping process. This is substantiated by the fact that: (i) plots of α vs. $1/T$ extrapolate to zero or very small intercepts at $1/T = 0$; (ii) that estimated charge carrier mobilities are less than $10^{-2} cm^2/V\text{-sec}$ below 1000 K, and assume values of $2X10^{-5} cm^2/V\text{-sec}$ at room temperature; and (iii) that whereas the resistivities are enormously sensitive to stoichiometry, the Seebeck coefficients are not. [Other authorities disagree with such a view and postulate that charge carrier transport occurs in very narrow bands; however, we feel that their conclusions are based primarily on measurements of Li-doped NiO where the situation is quite different, since even very small additions of this dopant significantly alter the properties of the host lattice.[25]]

On the hopping model the slopes of the straight line portions of Fig. 3 are proportional to the dissociation energy ε_d required to remove one hole from the nickel ion vacancy to which it is bound in the ground state. The theoretical analysis leads to the result[26]

$$\alpha = e\,\varepsilon_d/kT + A \qquad (3)$$

where A is a small numerical constant. The recommended graphs in Fig. 3 for $\delta = 0$ and $\delta \approx 5X10^{-3}$ corresponds to Eq. (3) with $\varepsilon_d = 0.3$ eV and $A \approx 0.30$ or $\varepsilon_d = 0.2$ eV and $A \approx 0.18$ for Curves A or B respectively.

The above model also leads to the following schematic expression for the conductivity $\sigma \equiv \rho^{-1}$:

$$\sigma = ne\mu = n_o e\mu_o \exp\{(-\varepsilon_n + \varepsilon_\mu(T))/kT\} \qquad (4)$$

wherein n is the charge carrier density, μ the mobility, e the electronic charge, ε_n and ε_μ the charge carrier density activation and mobility activation energies. This last quantity is given by $\varepsilon_\mu = \varepsilon_c - \varepsilon_m(T)$, where ε_c is

the energy required to bring the initial and final sitesinto energetic coincidence so that a charge transfer between these sites may occur when complete magnetic order prevails, and $\varepsilon_m(T)$ is the contribution of magnetic disorder which adds to the energy of the charge carrier and therefore diminishes the overall energy required for coincidence. The actual theoretical expression is rather complicated; interested readers should consult Ref. 4 for details. The recommended curve C in Fig. 1 for $\delta = 5X10^{-3}$ was based on calculations involving Eq. 4, with a variety of required input parameters taken from the literature. No such parameters are available for the strictly stoichiometric compound ($\delta = 0$); hence the upper limiting curve A of Fig. 1 is provisionally adopted for single crystals with nearly perfect stoichiometry.

We now turn to a consideration of Fig. 4. Here again, considerable caution is required in acceptance of data for polycrystalline samples. It is generally thought that Seebeck coefficients are not very sensitive to the state of subdivision of specimens; nevertheless, when the properties of surface layers differ appreciably from those of the bulk, Eq. (1) applies; Seebeck coefficients may be drastically altered for cases where the surface or boundary conductivity considerably exceeds that of the bulk of the grains. Curves 11-16 of Fig. 4 appear to be characteristic of polycrystalline materials where grain boundary effects are dominant. Most of the remaining graphs are relatively temperature independent, as would be the case if carrier transport occurred by a hopping process with a constant density of charge carriers. It is of interest that α falls in the range 0.2 to 1.6 mV/deg for polycrystalline samples, as compared to 0.1 to 2.0 mV/deg for single crystals. The recommended curves are the same as those given in Fig. 3.

Measurement information on the Seebeck coefficients of single crystal NiO is displayed in Table 7, and the experimental results are shown in Table 8.

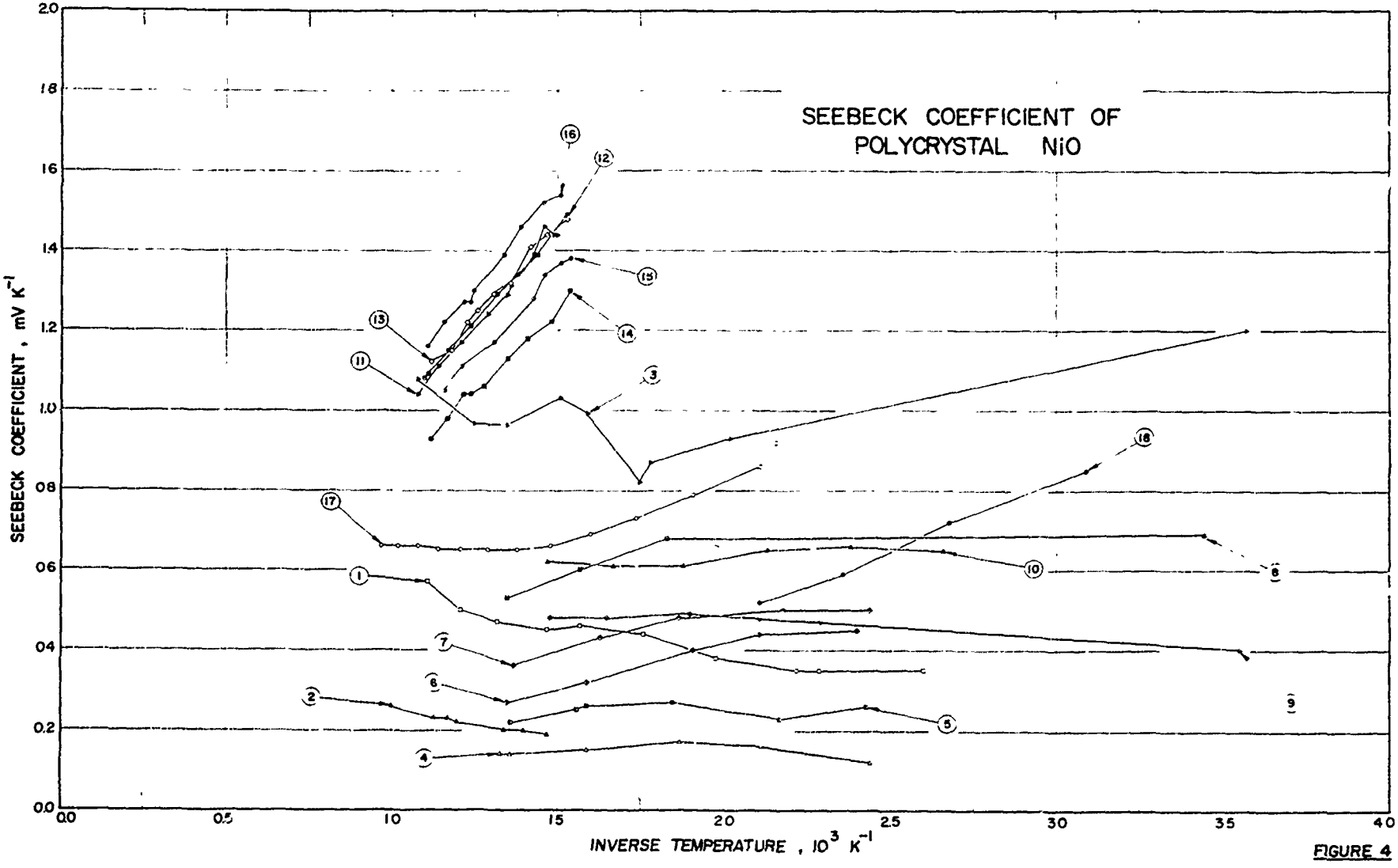
SEEBECK COEFFICIENT OF
POLYCRYSTAL NiO
SEEBECK COEFFICIENT , mV K⁻¹
INVERSE TEMPERATURE , 10³ K⁻¹
2.0
1.8
1.6
1.4
1.2
1.0
0.8
0.6
0.4
0.2
0.0
0.0
0.5
1.0
1.5
2.0
2.5
3.0
3.5
4.0
16
12
15
13
14
11
3
17
18
1
10
8
7
6
2
9
5
4

FIGURE 4

TABLE 7. MEASUREMENT INFORMATION ON THE SEEBECK COEFFICIENT (THERMOELECTRIC POWER) OF SINGLE CRYSTAL $Ni_{1-\delta}O$

Cur. No.	Ref. No.	Author(s)	Year	Method Used	Temp. Range, K	Name and Specimen Designation	Composition (weight percent), Specifications, and Remarks
1	29	Austin, I. G., Springthorpe, A. J., Smith, B. A., and Turner, C. E.	1967		250-388		Single crystals made by arc-transfer process, T_N=523 K. Indium or silver paste used as contact material. Differential thermocouple pressed into grooves in ends of sample.
2	29	Austin, I. G., Springthorpe, A. J., Smith, B. A. and Turner, C. E.	1967		246-1190		Same as for Curve 1, this page.
3	13	Osburn, C. M. and Vest, R. W.	1971		678-886		Single crystals manufactured by Argonne National Laboratories. Electrical resistivity measurements also reported.
4	40	Melik-Davtyan, R. L., Shvartsenau, N. F., and Shelykh, A. I.	1966		473-1024		Single crystals prepared by A. A. Popova, Institute of Crystallography AN SSSR. Measured in air w.r.t. Pt.
5	4	Keem, J. E.	1976		300-562		Single crystals prepared by arc-transfer technique. Measured in air.
6	4	Keem, J. E.	1976		300-846		Same as above.
7	4	Keem, J. E.	1976		300-846		Same as above.
8	4	Keem, J. E.	1976		300-846		Same as a e.
9	4	Keem, J. E.	1976		410-846		Same as above.
10	4	Keem, J. E.	1976		410-846		Same as above.

TABLE 8. TABULATION OF MEASURED SEEBECK COEFFICIENTS (THERMOELECTRIC POWER) OF SINGLE CRYSTAL $Ni_{1-\delta}O$

[Temperature, $10^3/T$, K^{-1}; α, mV/K]

$\frac{10^3}{T}$	α
CURVE 1	
2.58	1.432
2.62	1.482
2.66	1.526
2.70	1.559
2.72	1.599
2.75	1.649
2.79	1.699
2.83	1.751
2.85	1.803
2.89	1.839
2.94	1.893
2.98	1.945
3.02	1.985
3.07	2.000
3.14	1.993
3.20	1.967
3.24	1.935
3.48	1.666
3.55	1.611
3.63	1.518
3.85	1.274
4.00	1.123
CURVE 2	
0.84	0.096
0.85	0.186
0.90	0.315
0.99	0.457
1.09	0.532
1.19	0.571
1.28	0.619
1.39	0.665
1.48	0.718
1.58	0.770
1.67	0.809
1.77	0.856
1.86	0.894
1.91	0.931
1.95	0.960
1.99	0.986
2.11	1.081
2.62	1.447

$\frac{10^3}{T}$	α
CURVE 2 (cont.)	
2.66	1.464
2.69	1.490
2.72	1.514
2.75	1.548
2.80	1.572
2.84	1.612
2.88	1.642
2.94	1.651
2.99	1.665
3.04	1.660
3.09	1.652
3.14	1.628
3.18	1.595
3.21	1.560
3.28	1.458
3.34	1.402
3.35	1.364
3.47	1.231
3.52	1.176
3.57	1.111
3.67	0.988
3.73	0.904
3.80	0.869
3.86	0.770
4.00	0.598
4.06	0.544
CURVE 3	
1.128	0.355
1.166	0.355
1.189	0.360
1.342	0.379
1.475	0.379
CURVE 4	
2.114	1.116
1.912	1.016
1.745	0.949
1.605	0.902
1.486	0.860
1.383	0.825
1.294	0.786
1.215	0.756

$\frac{10^3}{T}$	α
CURVE 4 (cont.)	
1.145	0.733
1.083	0.708
1.028	0.685
0.977	0.662
CURVE 5	
1.67	0.78
1.77	0.84
1.83	0.84
2.00	0.89
2.11	0.90
2.23	1.08
2.35	1.07
2.62	1.16
3.03	1.21
3.12	1.30
CURVE 6	
3.33	1.3
2.66	1.14
2.36	0.99
2.00	0.89*
1.90	0.7
CURVE 7	
3.37	0.97
3.33	0.95
3.13	0.94
2.94	0.84
2.90	0.92
2.88	0.91
2.81	0.95
2.73	0.81
2.54	0.86
2.47	0.88
2.38	0.80
2.28	0.78
2.23	0.81
2.19	0.80
2.16	0.80
2.09	0.73
2.05	0.72
1.99	0.62

$\frac{10^3}{T}$	α
CURVE 7 (cont.)	
1.94	0.65
1.86	0.62
1.77	0.59
CURVE 8	
1.82	0.71
1.84	0.66
1.85	0.70
1.91	0.76
1.95	0.77
1.98	0.75
2.08	0.83
2.24	0.90
2.36	0.96
2.54	0.915
2.70	0.92
2.77	0.965
2.86	1.10
3.39	1.20
CURVE 9	
2.439	0.84
2.222	0.76
1.961	0.65
1.182	0.58
CURVE 10	
2.46	2.8*
2.44	2.33*
2.41	2.26*
2.38	1.28
2.36	1.13
2.34	1.10
2.30	1.06
2.23	1.02
2.11	1.00
2.06	0.97
2.04	1.00
1.94	0.99
1.90	0.93
1.87	0.95
1.83	0.94
1.79	0.92

$\frac{10^3}{T}$	α
CURVE 10 (cont.)	
1.69	0.90

*Not shown in figure

TABLE 9. MEASUREMENT INFORMATION ON THE SEEBECK COEFFICIENT (THERMOELECTRIC POWER) OF POLYCRYSTAL $Ni_{1-\delta}O$

Cur. No.	Ref. No.	Author(s)	Year	Method Used	Temp. Range, K	Name and Specimen Designation	Composition (weight percent), Specifications, and Remarks
1	28	Parravano, G.	1955		375-895		Sample prepared by thermal decomposition of solution of c.p. nitrates. ground, and fired in air for 4 h at 1173 K. Contacts were Pt foil. Measured in air, w.r.t. Pt.
2	13	Osburn, C. M. and Vest, R. W.	1971		682-1000		Samples obtained from Argonne National Laboratories.
3	41	van Houten, S.	1960		280-919		Bars or discs. $NiCO_3$ fired at 1173 K, milled, and hydrostatically pressed at 10 tons/cm^2. Fired in air at 1823 K. Cooled from 1073 K in N_2. Density 88-95% of maximum. Measured in air w.r.t. Pt.
4	42	Nachman, M., Cojocaru, L. N., and Rîbco, L. V.	1965		410-750	A	Cylindrical sample. Thermal decomposition of $NiCO_3$ at 873 K. Pressed at 1.5 t/cm^2. Heated in air for 20 h at decomposition temperature. Density 76.5% of maximum. T_N=523 K. Contacts were Pt. Measured in air w.r.t. Pt.
5	42	Nachman, M., Cojocaru, L. N., and Rîbco, L. V.	1965		411-734	B	Same as above except decomposition temperature was 973 K.
6	42	Nachman, M., Cojocaru, L. N., and Rîbco, L. V.	1965		416-738	C	Same as above except decomposition temperature was 1073 K and density 81.0% of maximum.
7	42	Nachman, M., Cojocaru, L. N., and Rîbco, L. V.	1965		409-730	D	Same as above except decomposition temperature was 1173 K and density 84.0% of maximum.
8	42	Nachman, M., Cojocaru, L. N., and Rîbco, L. V.	1965		291-740	E	Same as above except decomposition temperature was 1273 K and density 87.0% of maximum.
9	49	Dereń, J. and Ziółkowski, J.	1966		281-673		Measured in nitrogen at 280 mm Hg pressure.
10	49	Dereń, J. and Ziółkowski, J.	1966		375-679		Measured in air at 600 mm Hg pressure.
11	45	Wright, R. W. and Andrews, J. P.	1949		667-923	B_1	Nickel foil oxidized at 1273 K for 30 h. Contacts silver. Measured in air w.r.t. Pt.
12	45	Wright, R. W. and Andrews, J. P.	1949		652-902	B_2	Sample from same batch as the above. Same procedure.
13	45	Wright, R. W. and Andrews, J. P.	1949		652-886	C	Sample from same batch as the above. Same procedure.
14	45	Wright, R. W. and Andrews, J. P.	1949		645-980	D	Sample from same batch as the above. Same procedure.

TABLE 9. MEASUREMENT INFORMATION ON THE SEEBECK COEFFICIENT (THERMOELECTRIC POWER) OF POLYCRYSTAL $Ni_{1-\delta}O$ (continued)

Cur. No.	Ref. No.	Author(s)	Year	Method Used	Temp. Range, K	Name and Specimen Designation	Composition (weight percent), Specifications, and Remarks
15	45	Wright, R. W. and Andrews, J. P.	1949		647-857	E	Sample from same batch as above. Same procedure.
16	45	Wright, R. W. and Andrews, J. P.	1949		660-899	G	Sample from same batch as the above. Same procedure.
17	40	Melik-Davtyan, R. L., Shvartsenau, N. F., and Shelykh, A. I.	1966		463-1023		Nickel nitrate dried at 393-423 K, roasted for 2 h at 1573 K and converted into NiO. Measured in air w.r.t. Pt.
18	48	Schlosser, E. G.	1961		323-473		Thermal decomposition of $Ni(NO_3)_2$ for 5 h at 1273 K, washed in H_2O, then heated again to 1273 K for 5 h; pressed NiO powder. Measured in air w.r.t. Pt.

TABLE 10. TABULATION OF MEASURED SEEBECK COEFFICIENTS (THERMOELECTRIC POWER) OF POLYCRYSTAL $Ni_{1-\delta}O$

[Inverse Temperature, $10^3/T$, K^{-1}; Seebeck Coefficient, α, mV/K]

$\frac{10^3}{T}$	α
CURVE 1	
2.660	0.359
2.294	0.352
2.227	0.359
1.988	0.389
1.761	0.440
1.575	0.460
1.474	0.458
1.325	0.471
1.217	0.503
1.117	0.571
CURVE 2	
1.000	0.263
1.132	0.234
1.170	0.234
1.200	0.223
1.343	0.204
1.400	0.203
1.470	0.192
CURVE 3	
3.570	1.209
2.026	0.931
1.780	0.875
1.751	0.820
1.599	0.994
1.510	1.056
1.357	0.962
1.253	0.966
1.088	1.086
CURVE 4	
2.440	0.127
2.177	0.162
1.871	0.170
1.590	0.150
1.360	0.148
1.334	0.146
CURVE 5	
2.435	0.260
2.175	0.236
CURVE 5 (cont.)	
1.850	0.276
1.590	0.263
1.562	0.253
1.363	0.225
CURVE 6	
2.405	0.458
2.124	0.447
1.911	0.401
1.599	0.320
1.355	0.272
CURVE 7	
2.444	0.509
2.182	0.507
1.870	0.480
1.631	0.432
1.370	0.364
CURVE 8	
3.440	0.699
1.830	0.680
1.572	0.603
1.352	0.532
CURVE 9	
3.558	0.408
2.299	0.473
2.114	0.484
1.908	0.491
1.656	0.486
1.486	0.486
CURVE 10	
2.666	0.659
2.387	0.664
2.132	0.652
1.880	0.613
1.672	0.616
1.473	0.623
CURVE 11	
1.083	1.043
1.085	1.067*
1.149	1.119
1.212	1.170
1.291	1.248
1.353	1.295
1.367	1.317
1.433	1.398
1.465	1.461
1.491	1.441
1.500	1.441
CURVE 12	
1.109	1.082
1.114	1.096
1.179	1.153
1.241	1.210
1.324	1.291
1.382	1.345
1.398	1.363*
[illegible]	1.399
1.533	1.492
CURVE 13	
1.129	1.122
1.185	1.156
1.197	1.185*
1.239	1.230
1.261	1.257
1.319	1.291
1.365	1.347
1.428	1.418
1.472	1.447
1.534	1.483
CURVE 14	
1.123	0.932
1.171	0.985
1.220	1.044
1.249	1.045
1.284	1.067
1.353	1.138
1.411	1.183
CURVE 14 (cont.)	
1.482	1.227
1.549	1.302
CURVE 15	
1.167	1.050
1.219	1.119
1.317	1.179
1.432	1.288
1.467	1.347
1.510	1.376
1.545	1.385
CURVE 16	
1.112	1.169
1.167	1.223
1.226	1.274
1.247	1.277
1.250	1.307
1.340	1.396
1.398	1.469
1.460	1.520
1.514	1.547
CURVE 17	
2.160	0.921
2.114	0.867
1.912	0.793
1.745	0.731
1.605	0.690
1.486	0.665
1.383	0.658
1.294	0.658
1.215	0.658
1.145	0.658
1.083	0.662
1.018	0.662
0.977	0.662
CURVE 18	
3.096	0.856
2.681	0.723
2.364	0.598
2.114	0.521

[illegible] figure

The corresponding information for polycrystal NiO is provided in Tables 9 and 10 respectively.

3.3 Heat Capacity

Recommended values for the heat capacity of NiO are collected in Table 11. Itsconstruction will be commented on below.

Heat capacity measurements at constant pressure are shown as plots of C_p vs T in Fig. 5. The results of investigations are nicely concordant, except in the temperature region near T_N, where the measurement depends not only on the manner in which the sample is passed through the Néel point but also on the precise variation of long and short-range magnetic order as a function of temperature. Heat capacity properties outside the anomalous region are insensitive to the state of subdivision, impurity content, and stoichiometry of the sample. According to standard theory, the gradual disappearance of magnetic order on heating should lead to a second-order transition, which, in the simplest cases, manifests itself as a λ-anomaly in the heat capacity.[19] Such anomalies have been observed in most cases, but in one particular instance a much sharper peak has been reported (Curve 4) which is more reminiscent of a first-order transition.

Above the Néel point, T_N = 523 K, the heat capacity C_p reaches an asymptotic value of 0.172 cal/g-deg which lies higher by 3% than the anticipated Dulong and Petit value for the heat capacity of constant volume, C_V = 11.92 cal/mole-deg for NiO; this discrepancy is expected on the basis of Eq. (2).

The recommended curve is an average of the various reported values outside the temperature range of the C_p anomaly, for which no recommendation is possible for reasons outlined above.

TABLE 11

RECOMMENDED VALUES FOR THE SPECIFIC HEAT AT CONSTANT PRESSURE OF NiO

Temperature, K	Specific Heat, cal g^{-1} K^{-1}
0	0.001
50	0.011
100	0.044
150	0.080
200	0.107
300	0.141
400	0.168
480	0.194
500	0.204
505	0.211
510	0.230
545	0.226
550	0.205
560	0.189
580	0.179
600	0.175
700	0.172
800	0.172
900	0.172
1000	0.172

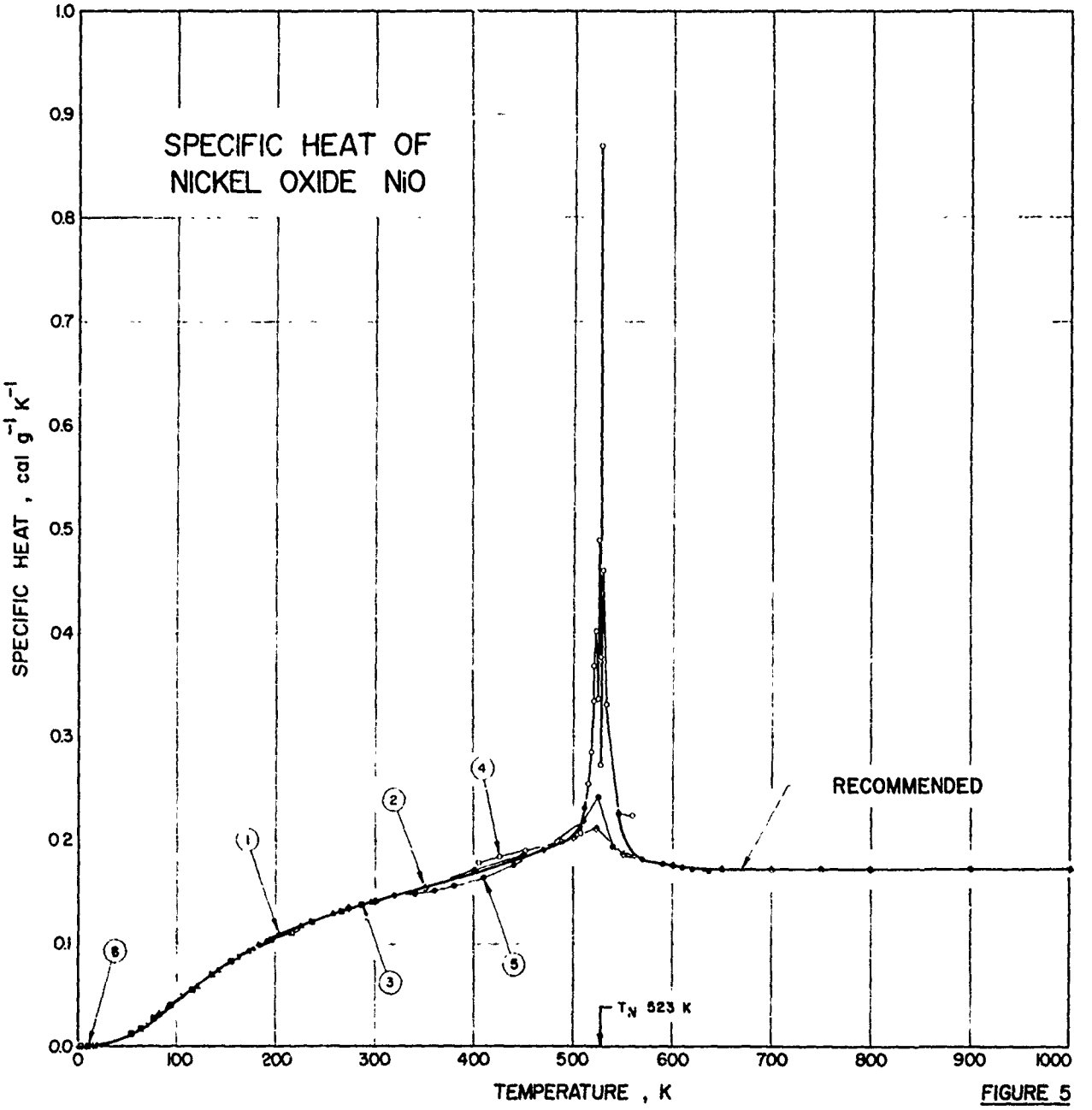
SPECIFIC HEAT OF
NICKEL OXIDE NiO
SPECIFIC HEAT , cal g⁻¹ K⁻¹
TEMPERATURE , K
RECOMMENDED
T_N 523 K
1.0
0.9
0.8
0.7
0.6
0.5
0.4
0.3
0.2
0.1
0.0
0
100
200
300
400
500
600
700
800
900
1000
1
2
3
4
5
6

FIGURE 5

The experimental data of Fig. 5, after subtraction of the anomalous portion due to the second order transition, may be interpreted within the framework of the Debye theory, according to which for each elementary lattice constituent the molar heat capacity reads:

$$\tilde{C}_V = 9\ Nk\ \left(\frac{T}{\theta}\right)^3 \{4\mathcal{D}(\tfrac{\theta}{T}) + T\mathcal{D}'(\tfrac{\theta}{T})\} \tag{5}$$

in which N is Avogadro's number and

$$\mathcal{D}\ (\tfrac{\theta}{T}) \equiv \int_0^{\theta/T} \frac{x^3}{e^x - 1}\, dx, \quad \theta \equiv h\nu_m/k \tag{6}$$

θ being termed the Debye temperature, which is related to the maximum lattice vibration frequency ν_m as shown above. It is worth noting that at low temperatures $T \ll \theta$, the above relation approximates to $\tilde{C}_V \approx (12/5)\pi^4 Nk(T/\theta)^3$, whereas at high temperatures it approaches the Dulong and Petit value $\tilde{C}_V \approx 3\ Nk$ per atomic unit. The above quantities must be doubled to take account of the fact that NiO contains two atomic species per formula unit. Since tabulations of $\mathcal{D}(\theta/T)$ are available, it is possible to test the data for their fit to Eq. (5); it is found that reasonable though not excellent agreement may be attained in the range $0 < T < 250$ K with a value of $\theta = 580$ K. Obviously such a fit cannot cope with the λ-anomaly; also, above 300 K the difference between $\tilde{C}_p$ and $\tilde{C}_V$ becomes sufficiently noticeable so that values calculated according to Eq. (5) are expected to lie by several percent below the measured $\tilde{C}_p$ values. Finally, one should recall that the lattice symmetry changes as the NiO passes through the antiferromagnetic ordering temperature: one would thus expect θ for $T > T_N$ to be different from θ for $T < T_N$.

Information on measurement techniques of heat capacity determinations is accumulated in Table 12; the actual data are tabulated in Table 13.

TABLE 12. MEASUREMENT INFORMATION ON THE CONSTANT PRESSURE SPECIFIC HEAT OF NiO

Cur. No.	Ref. No.	Author(s)	Year	Method Used	Temp. Range, K	Name and Specimen Designation	Composition (weight percent), Specifications, and Remarks
1	50	Seltz, H., DeWitt, B. J., McDonald, H. J.	1940		68-298.1		Chemical pure NiO powder with less than 0.2% impurities dried for several days at 373 K; molal heat capacity in calories per °C given in graphical form.
2	51	Tomlinson, J. R., Domash, L., Hay, R. G., and Montgomery, C. W.	1954		300-1100.0		Thermal decomposition of $Ni(NO_3)_2 \cdot 8H_2O$; maintained after decomposition at 1273 K for 8 h; T_N=523.
3	52	King, E. G.	1956		50-298		Thermal decomposition at 1273 K for 9 days of $Ni(NO_3)_2$;synthesized from $Ni(NO_2)_2 \cdot 8H_2O$ and $NiSO_4 \cdot 8H_2O$ dissolved in water by precipitation using NH_3OH and CO_2 gas; heat capacity data given in graphical form.
4	53	Zhuze, V. P., Novruzov, O. N., and Shelykh, A.I.	1969		400-570		Single crystal grown by flame fusion technique; T_N=522 K; heat capacity data given in graphical form; relative heat capacity measured by pulse technique normalized to literature value at 400 K. Very large, very narrow peak observed (65 cal per mole-deg.) at 522 K.
5	21	Lewis, F. B., and Saunders, N. H.	1973		510-650	NiO(I)	Single crystal (100) direction; 4x4x25 mm; grown by flame fusion technique; T_N=525 K; heat capacity data given in graphical form; measured using a differential scanning calorimeter comparing to Al_2O_3 and assuming C_p "approximately constant over the temperature excursion employed (usually approximately 10 K)."
6	54	White, H. W.	1974		3.2-18.75		Single crystal, 99.99% pure; rod 12 mm diameter, 40 mm long; Θ_D=595±20 K; data presented in graphical form; heat pulse technique used.

TABLE 13. TABULATION OF MEASURED SPECIFIC HEATS OF NiO

[Temperature, T, K; Specific Heat, C_p, cal $g^{-1}K^{-1}$]

T	C_p
CURVE 1	
68.05	2.151E-02
71.96	2.556E-02*
78.19	2.925E-02*
82.07	3.217E-02
85.89	3.515E-02*
86.70	3.540E-02*
91.08	3.919E-02
94.42	4.141E-02*
96.32	4.416E-02*
103.1?	4.944E-02
111.70	5.481E-02*
115.71	5.679E-02*
120.33	5.977E-02
131.13	6.692E-02*
141.72	7.469E-02
150.08	7.937E-02*
151.86	8.058E-02*
162.37	8.756E-02
168.09	9.204E-02*
172.61	9.296E-02
181.22	9.854E-02
183.01	1.004E-01
190.75	1.023E-01
204.20	1.087E-01
213.13	1.143E-01*
225.34	1.184E-01
235.37	1.217E-01*
247.81	1.275E-01*
257.49	1.305E-01
277.20	1.375E-01*
286.32	1.396E-01*
296.68	1.413E-01
CURVE 2	
273.16	1.357E-01
300.00	1.415E-01
350.00	1.547E-01
400.00	1.700E-01
450.00	1.865E-01
500.00	2.036E-01
523.16	2.118E-01
550.00	1.861E-01
600.00	1.753E-01
650.00	1.728E-01

T	C_p
CURVE 2 (cont.)	
700.00	1.728E-01
750.00	1.728E-01
800.00	1.728E-01
850.00	1.728E-01*
900.00	1.728E-01
950.00	1.728E-01*
1000.00	1.728E-01
CURVE 3	
54.28	1.205E-02
58.92	1.488E-02*
63.49	1.795E-02
68.10	2.118E-02*
72.47	2.433E-02*
76.74	2.745E-02
80.22	3.009E-02*
83.81	3.271E-02*
94.66	4.090E-02
104.97	4.871E-02*
115.57	5.506E-02
124.60	6.279E-02*
135.88	7.053E-02
145.85	7.679E-02*
155.86	8.327E-02
165.78	8.886E-02*
175.84	9.424E-02*
185.78	9.941E-02*
195.94	1.042E-01
206.13	1.089E-01*
216.19	1.132E-01
225.85	1.173E-01*
236.07	1.211E-01
245.63	1.246E-01*
256.79	1.285E-01*
266.15	1.318E-01
276.01	1.349E-01*
286.43	1.381E-01
295.94	1.422E-01*
CURVE 4	
404.	1.780E-01
413.	1.820E-01*
425.	1.847E-01

T	C_p
CURVE 4 (cont.)	
435.	1.861E-01*
452.	1.901E-01
473.	1.874E-01*
474.	1.941E-01*
488.	1.994E-01
499.	1.994E-01*
507.	2.075E-01
511.	2.316E-01
514.	2.543E-01
517.	2.342E-01*
517.	2.503E-01*
518.	2.851E-01
519.	3.052E-01*
519.	3.212E-01*
520.	3.346E-01
520.	3.681E-01
522.	4.016E-01
523.	3.360E-01
523.	4.364E-01*
523.	4.404E-01*
525.	4.899E-01
526.	3.761E-01
527.	8.700E-01
527.	2.731E-01
528.	4.671E-01*
529.	4.604E-01
529.	4.136E-01*
529.	3.614E-01*
529.	3.065E-01*
529.	2.650E-01*
532.	3.734E-01*
532.	2.597E-01*
533.	3.319E-01
533.	2.717E-01*
546.	2.262E-01
548.	2.449E-01*
548.	2.396E-01*
552.	2.275E-01*
559.	2.249E-01
CURVE 5	
3.20	2.075E-06
3.27	2.248E-06*
3.59	2.833E-06*

T	C_p
CURVE 5 (cont.)	
3.89	3.549E-06*
3.94	3.709E-06*
4.48	5.596E-06*
4.79	6.523E-06*
4.83	7.035E-06*
5.02	7.770E-06*
5.21	8.346E-06*
5.32	9.209E-06*
5.56	1.046E-05*
5.69	1.049E-05*
5.83	1.193E-05*
6.18	1.417E-05*
6.20	1.365E-05*
6.51	1.567E-05*
6.60	1.695E-05*
7.04	1.973E-05*
7.27	2.256E-05*
7.74	2.705E-05*
8.21	3.185E-05*
8.67	3.716E-05*
8.90	4.080E-05*
9.63	4.806E-05*
10.45	6.040E-05
10.77	7.211E-05*
11.51	8.758E-05*
12.22	1.037E-04*
12.90	1.198E-04*
13.59	1.426E-04*
13.85	1.521E-04*
14.63	1.794E-04*
15.33	1.985E-04*
16.85	2.731E-04*
17.86	3.201E-04*
18.75	3.729E-04*
CURVE 6	
320.	1.472E-01
330.	1.481E-01*
340.	1.493E-01
350.	1.507E-01*
360.	1.527E-01
370.	1.541E-01*
380.	1.562E-01
390.	1.585E-01*

T	C_p
CURVE 6 (cont.)	
400.	1.613E-01*
410.	1.648E-01
420.	1.632E-01*
430.	1.722E-01*
440.	1.761E-01
450.	1.808E-01*
460.	1.859E-01*
470.	1.916E-01
480.	1.964E-01*
490.	2.035E-01*
500.	2.119E-01*
510.	2.195E-01
520.	2.334E-01*
525.	2.422E-01
530.	2.047E-01*
540.	1.945E-01
550.	1.887E-01*
560.	1.851E-01*
570.	1.823E-01
580.	1.801E-01*
590.	1.785E-01
600.	1.763E-01
610.	1.744E-01
620.	1.732E-01
630.	1.720E-01
637.	1.715E-01

*Not shown in figure

3.4 Thermal Conductivity

Recommended values for the thermal conductivity are shown in Table 14; comments concerning these are provided below.

Thermal conductivity (κ) curves are shown in Fig. 6 as plots of log κ vs log T. Various sets of data are widely different, as is expected from the fact that κ is very sensitive to the state of subdivision of the sample. Nevertheless, the general character of the data follows the anticipated pattern. The thermal conductivity passes through a maximum; at higher temperatures κ is governed primarily through the mean free path, as determined by phonon-phonon scattering processes; since with rising temperature the phonon density increases according to the Bose-Einstein law, the mean free path decreases and κ diminishes correspondingly.

The only really effective phonon collisions are the so-called umklapp processes[27] which require that at least one of the phonons have a wave vector greater than half of the maximum possible value, i.e., greater than $(1/2)\nu_m = (1/2)k\ \theta/h$, where θ is the Debye temperature introduced earlier. The probability of encountering such phonons at temperature T is proportional to $\exp(-h\nu_m/2\ kT) = \exp(-\theta/2T)$. To find a second phonon of an appropriate wave number so as to make an umklapp process feasible involves a probability which varies as $(\theta/T)^3$. Therefore, the anticipated temperature behavior for κ in this regime is

$$\kappa = \kappa_0 (T/\theta)^3 \exp(\theta/2T) \qquad (7)$$

where κ_0 is a parameter independent of κ and T.

At lower temperatures the phonon density becomes sufficiently low so that the mean free path, ℓ, of phonons increases to a point where it is limited by the average distance between defects or by the grain size in the specimens. In this region the thermal conductivity is given by

TABLE 14

PROVISIONALLY RECOMMENDED VALUES FOR THE THERMAL CONDUCTIVITY OF NiO IN THE RANGE 3-700 K

Temperature, K	Thermal Conductivity, W cm^{-1} K^{-1}
2.8	0.0172
4	0.0512
6	0.163
8	0.352
10	0.615
15	1.45
20	2.26
25	2.95
30	3.49
35	3.82
40	3.97
45	4.01
50	3.97
55	3.84
60	3.54
80	2.54
100	1.90
150	1.08
200	0.640
250	0.338
300	0.202
400	0.115
500	0.0785
700	0.0455

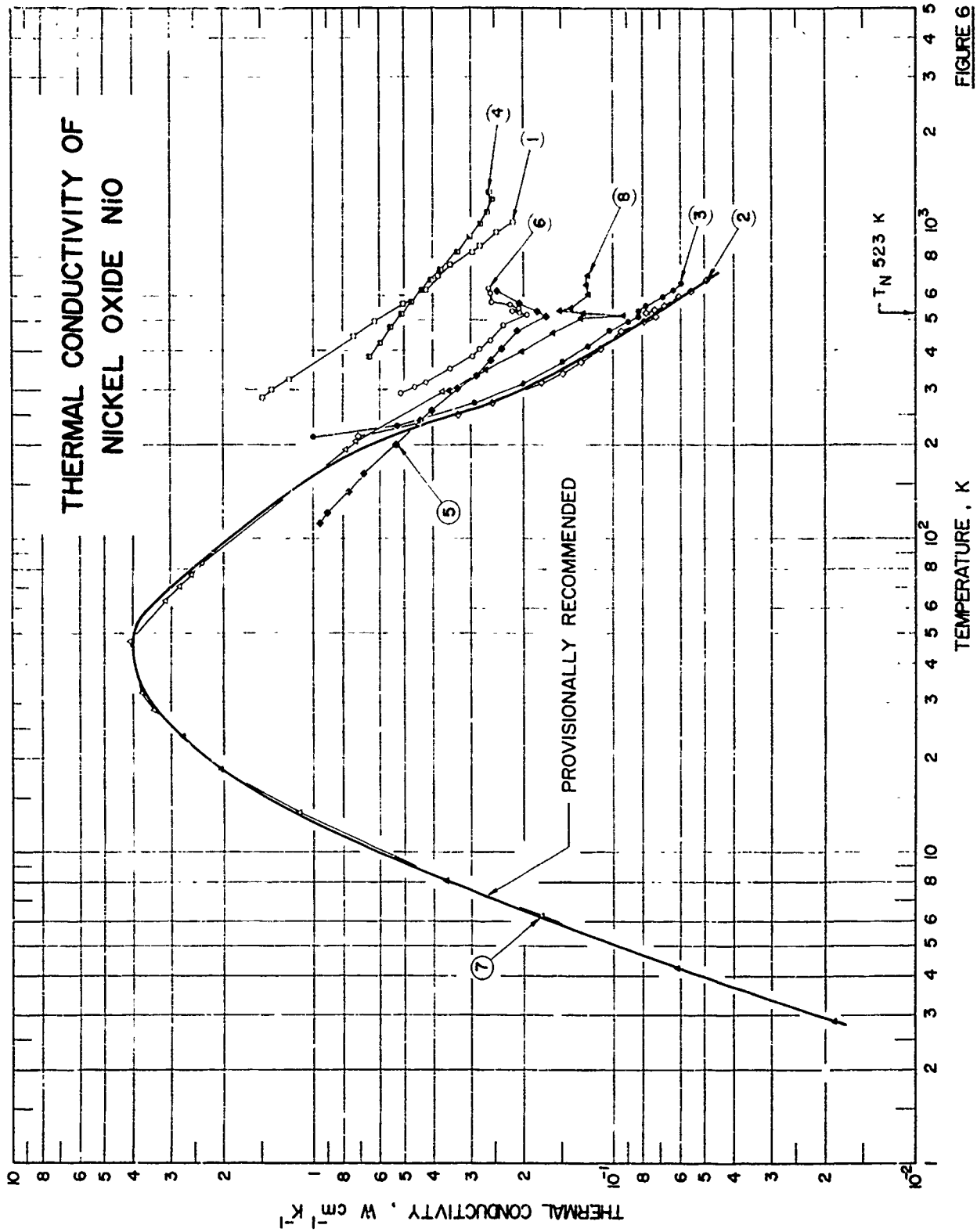
THERMAL CONDUCTIVITY OF
NICKEL OXIDE NiO
PROVISIONALLY RECOMMENDED
T_N 523 K
THERMAL CONDUCTIVITY , W cm^{-1} K^{-1}
TEMPERATURE , K
(1)
(2)
(3)
(4)
(5)
(6)
(7)
(8)

FIGURE 6

$$\kappa = \frac{1}{3} \tilde{C}_V \bar{v}_s \ell/\tilde{V} \qquad (8)$$

where $\tilde{C}_V$ is the molar heat capacity, $\bar{v}_s$ the sound velocity, and $\tilde{V}$ the molar volume, and ℓ, the mean free path. In the temperature range where (8) holds, $\bar{v}_s$ and ℓ are essentially constant, so that κ varies with T in the same manner as $\tilde{C}_V$. According to the preceding section, in this regime, $\tilde{C}_V = (12\pi^4 Nk/5\ \theta^3)T^3$, so that $\kappa \sim T^3$.

The data of Ref. 57 were found to be consistent with Eq. (7) for temperatures above the maximum in κ. The results below 20 K were fit to Eq. (8) with a mean free path of 30 microns. However, the θ value of 510 K required for a fit to the experimental κ is well below the θ value of 580 K used to fit the heat capacity result.

All data exhibit a kink in the vicinity of the Néel point. This may be ascribed to the fact that the lattice symmetry and dimension change slightly in the transition, thus altering the Debye temperature θ, and thereby, $\tilde{C}_V$. Furthermore, as will be seen shortly the mechanical properties of the lattice are also changed as the samples are heated through the Néel point; hence $\bar{v}_s$ changes as the magnetic order is altered. Both factors affect κ in the manner depicted in Fig. 6.

The provisionally recommended curve coincides with the data of Ref. 57 for $T < 20$ K and Ref. 55 for $T > 20$ K, as being representative for annealed single crystals of NiO. It should be clearly recognized that much more experimental work must be accumulated in the cryogenic temperature range before a reliable trend in the low temperature thermal conductivities can be established.

The measurement information for these experiments is provided in Table 15, and the tabulation of measurements is assembled in Table 16.

TABLE 15. MEASUREMENT INFORMATION ON THE THERMAL CONDUCTIVITY OF NiO

Cur. No.	Ref. No.	Author(s)	Year	Method Used	Temp. Range, K	Name and Specimen Designation	Composition (weight percent), Specifications, and Remarks
1	40	Melik-Davtyan, R. I., Shvartsenau, N. F., and Shelykh, A. I.	1966		283-1032		Nickel nitrate dried at 393-423 K, roasted at 1573 K and converted into NiO. Measured in air by steady-state method.
2	55	Shchelkotunov, V. A. and Danilov, V. N.	1971	→	211-670		Single crystal (100) direction; 6x6x6 mm; uncorrected for thermal expansion. Thermal resistivity data reported in graphical form; quasi-stationary monotonic temperature change technique checked by stationary state measurements and averaged over three specimens; minimum noted near the Neel point.
3	55	Shchelkotunov, V. A. and Danilov, V. N.	1971	→	211-654		Same as above. Same procedure except measured in (110) direction.
4	56	Kingery, W. D., Francl, J., Coble, R. L., and Vasilos, T.	1954	C	380-1294		Chemical pure NiO calcined at 1273 K, hydrostatically pressed, fired at 1773 K in an oxidizing atmosphere; d = 5.05 (gm/cm); uncorrected for thermal expansion; thermal conductivity reported in graphical form; both corrected for theoretical density and as measured; no minimum noted near the Néel point.
5	21	Lewis, F. B., and Saunders, N. H.	1973	L	112-620	NiO(I)	Single crystal (100) direction; 4x4x25 mm; grown by flame fusion technique T_N=525 K; data not corrected for thermal expansion; thermal conductivity data presented in graphical form; minimum noted near Neel point.
6	21	Lewis, F. B., and Saunders, N.H.	1973	L	291-633	NiO(III)	Same as NiO(I) except annealed at 1273 K for 24 h in CO_2 atmosphere.
7	57	Slack, G. A., and Newman, R.	1958	→	3-296		Single crystal rod 20 mm long, 5mm diameter; grown by flame fusion technique T_N=525 K, θ_D=410; uncorrected for thermal expansion; thermal conditions given in graphical form; measured by steady-state heat-flow method; inferred a phonon mean-free path of 30 microns.
8	53	Zhuze, V. P., Novruzov, O. N., Shelykh, A. I.	1969	→	297-694		Single crystal grown by flame fusion technique; T_N=522 K; uncorrected for thermal expansion; thermal diffusivity and heat capacity data given in graphical form; measured by pulse technique with yields at each temperature. Thermal diffusion time and a temperature rise; thus, knowing the sample size, density, and the heat capacity at one temperature the temperature dependence of the thermal conductivity and heat capacity may be calculated. This technique should be superior to other methods because only very small temperature changes (≤0.4 K) are required to make the measurement; hence, there is very little temperature averaging, and consequently, details on the temperature dependence of the thermal conductivity and heat capacity are not obliterated.

TABLE 16. TABULATION OF MEASURED THERMAL CONDUCTIVITIES OF NiO

[Temperature, T, K; Thermal Conductivity, <, watts $cm^{-1}K^{-1}$]

T	K
CURVE 1	
283	1.48
300	1.38
324	1.21
448	0.732
498	0.629
564	0.502
679	0.426
699	0.389
751	0.351
826	0.297
867	0.280
954	0.247*
982	0.239
1032	0.216
CURVE 2	
380	6.522E-01
423	6.068E-01
473	5.566E-01
523	5.112E-01
573	4.730E-01
623	4.396E-01
673	4.085E-01
723	3.799E-01
773	3.584E-01
823	3.368E-01
873	3.177E-01*
923	3.010E-01
973	2.891E-01*
1023	2.795E-01
1073	2.723E-01
1123	2.652E-01
1173	2.604E-01
1223	2.556E-01*
1273	2.532E-01*
1294	2.604E-01*
CURVE 3	
2.85	1.866E-02
4.24	6.151E-02
6.20	1.753E-01
8.03	3.622E-01
13.42	1.135E-00
18.45	2.051E-00
23.55	2.741E-00

T	K
CURVE 3 (cont.)	
28.51	3.427E-00
32.13	3.741E-00
47.09	4.102E-00
63.67	3.118E-00
70.45	2.805E-00
76.91	2.582E-00
83.17	2.371E-00
191.86	7.934E-01
205.58	7.261E-01
295.12	3.741E-01
CURVE 4	
297	3.570E-01
299	3.720E-01
333	3.077E-01
348	2.681E-01
373	2.317E-01*
375	2.427E-01*
378	2.278E-01*
399	2.037E-01
413	1.947E-01*
413	1.868E-01*
459	1.608E-01
462	1.466E-01*
465	1.600E-01*
481	1.482E-01*
492	1.430E-01*
499	1.300E-01
504	1.387E-01*
509	1.281E-01*
515	1.158E-01*
519	9.299E-02
520	1.021E-01
521	1.107E-01*
521	1.422E-01
523	1.277E-01*
526	1.399E-01*
528	1.462E-01*
537	1.509E-01*
543	1.383E-01*
547	1.470E-01*
552	1.352E-01*
560	1.391E-01*
562	1.304E-01*
584	1.261E-01*
601	1.222E-01

T	K
CURVE 4 (cont.)	
610	1.162E-01*
611	1.273E-01
651	1.249E-01
652	1.312E-01
665	1.139E-01*
694	1.233E-01*
CURVE 5	
211	7.140E-01
249	3.330E-01
271	2.560E-01
293	2.080E-01*
316	1.754E-01
339	1.493E-01
367	1.299E-01
405	1.111E-01
465	9.434E-02
491	8.264E-02
499	7.937E-02
506	7.751E-02
511	7.463E-02
515	7.299E-02*
520	7.407E-02
525	7.634E-02
529	7.874E-02*
535	7.634E-02*
540	7.353E-02
546	7.042E-02*
556	6.803E-02*
594	6.061E-02
620	5.587E-02
644	5.263E-02*
670	4.926E-02*
CURVE 6	
112	9.571E-01
121	9.057E-01
141	7.691E-01
162	6.839E-01
176	5.915E-01*
200	5.370E-01
239	4.425E-01
259	4.083E-01
267	3.845E-01*
301	3.372E-01

T	K
CURVE 6 (cont.)	
322	3.273E-01
333	2.897E-01*
338	2.779E-01
347	2.805E-01
374	2.582E-01
395	2.466E-01
405	2.371E-01
423	2.254E-01*
462	2.103E-01
488	1.963E-01*
515	1.686E-01
522	1.757E-01
527	1.640E-01*
539	1.807E-01*
545	1.923E-01*
564	2.079E-01
582	2.182E-01
620	2.466E-01
CURVE 7	
211	1.000E+00
230	5.263E-01
271	2.941E-01
355	2.000E-01
369	1.449E-01
411	1.220E-01
465	1.031E-01
495	8.929E-02
506	8.547E-02
511	8.264E-02*
516	8.000E-02*
521	7.752E-02*
528	8.000E-02*
535	8.264E-02*
542	8.065E-02
552	7.813E-02
564	7.636E-02
593	6.897E-02
625	6.369E-02
654	5.988E-02
CURVE 8	
291	5.164E-01
293	4.909E-01*
295	4.236E-01*

T	K
CURVE 8 (cont.)	
307	4.613E-01
318	4.236E-01
333	3.962E-01*
350	3.531E-01
366	3.155E-01*
372	3.341E-01*
381	2.964E-01*
389	3.169E-01*
399	2.958E-01*
405	2.824E-01
431	2.594E-01*
442	2.624E-01
483	2.344E-01
508	2.079E-01*
521	1.958E-01
523	2.023E-01
530	2.070E-01
537	2.192E-01
542	2.084E-01
561	2.218E-01
572	2.558E-01
584	2.517E-01
612	2.588E-01
633	2.624E-01

*Not shown in figure

3.5 Elastic Properties

Since only one set of measurements is available over a wide range of temperature, these must serve as provisional recommended values; smoothed values are assembled in Table 17.

A variety of elastic constants are plotted in their dependence on temperature in Fig. 7; these measurements were obtained on single crystals. As is seen, the experimenters report discontinuities or anomalous thermal variations near the Néel point for all elastic constants save C_{44}. The anomaly is to be expected since the second order transition is associated with magnetostriction effects which alter the structure and mechanical characteristics of the lattice. It is of interest that for some of the elastic constants the anomalies occur over a considerable temperature range well below the temperature T_N for which the heat capacity anomaly reaches its maximum value; this shows that structural relaxation effects begin to be noticeable before the total disappearance, on heating, of magnetic ordering effects.

Measurement information on elastic constants is assembled in Table 18 and the literature data are compiled in Table 19.

Young's modulus Y is shown as a function of temperature in Fig. 8. Of the two measurements the lower set is suspect because these measurements were carried out on untreated powdered specimens. The upper curve represents data taken on polycrystalline, sintered samples and is provisionally recommended. The recommended values are listed in Table 20; measurement information and literature values are exhibited in Tables 21 and 22 respectively.

TABLE 17

PROVISIONALLY RECOMMENDED VALUES FOR VARIOUS SETS OF NiO IN THE RANGE 4-710 K

Temperature, K	ELASTIC CONSTANT, 10^{12} dyne/cm^{-2}			
	$\frac{1}{2}(C_{11} - C_{12})$	$\frac{1}{3}(C_{11} + 2C_{12})$	$\frac{1}{2}(C_{11}+C_{12}+2C_{44})$	C_{44}
4	—	1.430	—	—
50	—	1.430	—	—
70	0.450	—	2.683	1.088
100	0.455	1.428	2.680	1.086
150	0.468	1.422	2.680	1.086
200	0.502	1.412	2.682	1.088
250	0.558	1.387	2.685	1.093
300	0.650	1.352	2.690	1.095
350	0.780	1.308	2.684	1.097
400	0.905	1.268	2.680	1.099
450	1.013	1.244	2.694	1.100
470	—	1.257	2.708	—
480	—	1.300	2.755	—
490	—	1.520	2.945	1.105
500	1.082	1.544	3.010	1.113
510	1.093	1.525	3.022	1.126
520	1.135	1.469	—	1.135
550	1.270	1.407	3.026	1.147
600	1.343	1.405	3.029	1.161
650	—	1.407	—	—
670	1.345	—	3.031	1.186
710	—	1.409	—	—

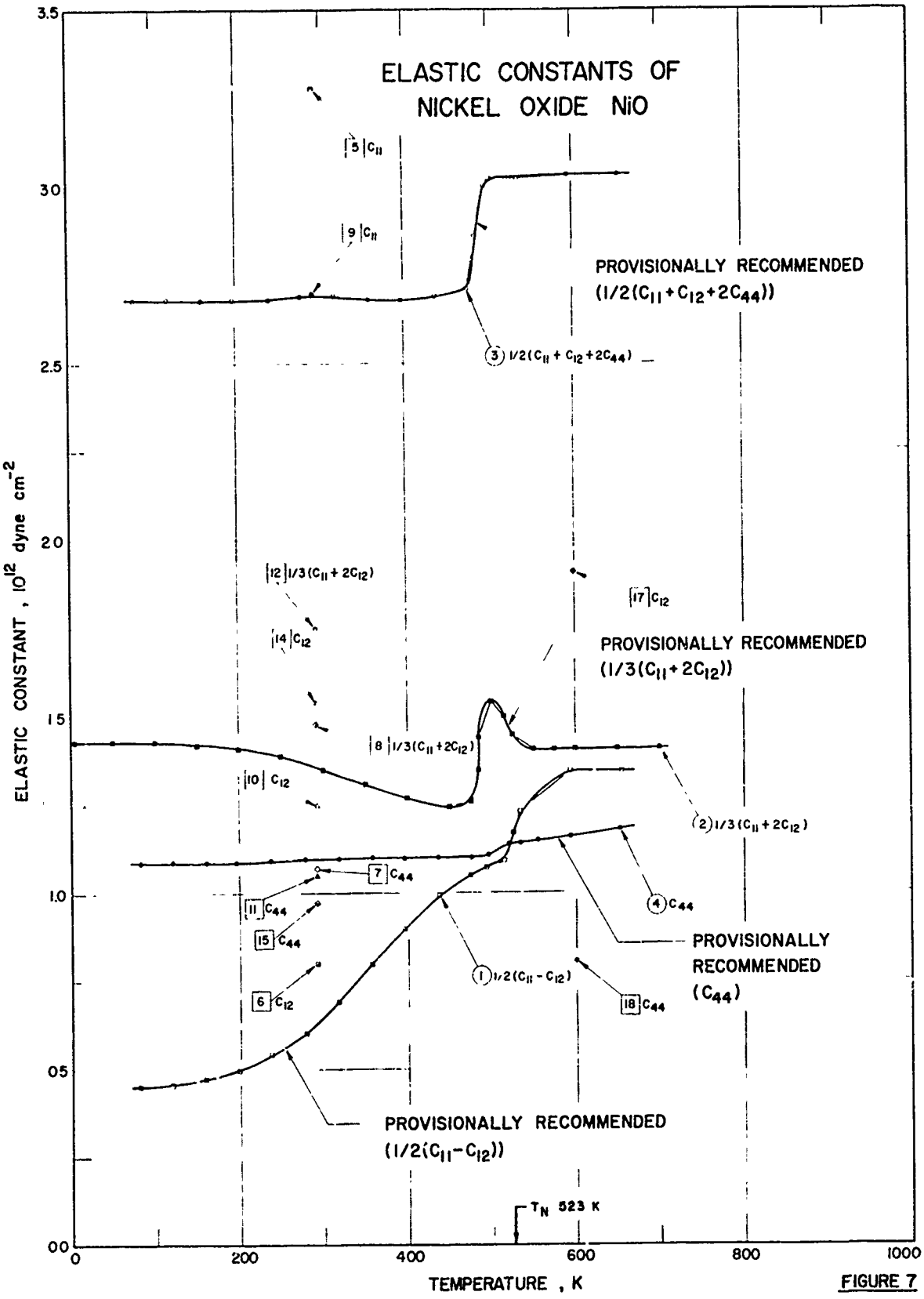
ELASTIC CONSTANTS OF
NICKEL OXIDE NiO
ELASTIC CONSTANT , 10^{12} dyne cm^{-2}
TEMPERATURE , K
3.5
3.0
2.5
2.0
1.5
1.0
0.5
0.0
0
200
400
600
800
1000
[5] C_{11}
[9] C_{11}
PROVISIONALLY RECOMMENDED
($1/2(C_{11}+C_{12}+2C_{44})$)
(3) $1/2(C_{11}+C_{12}+2C_{44})$
[12] $1/3(C_{11}+2C_{12})$
[14] C_{12}
[17] C_{12}
PROVISIONALLY RECOMMENDED
($1/3(C_{11}+2C_{12})$)
[8] $1/3(C_{11}+2C_{12})$
[10] C_{12}
(2) $1/3(C_{11}+2C_{12})$
[7] C_{44}
[11] C_{44}
[15] C_{44}
(4) C_{44}
PROVISIONALLY
RECOMMENDED
(C_{44})
(1) $1/2(C_{11}-C_{12})$
[6] C_{12}
[18] C_{44}
PROVISIONALLY RECOMMENDED
($1/2(C_{11}-C_{12})$)
T_N 523 K

FIGURE 7

TABLE 18. MEASUREMENT INFORMATION ON THE ELASTIC CONSTANTS OF NiO

Cur. No.	Ref. No.	Author(s)	Year	Method Used	Temp. Range, K	Name and Specimen Designation	Composition (weight percent), Specifications, and Remarks
1	18	du Plessis, P. de V., van Tonder, S. J., and Alberts, L.	1971		80-655		Single crystal cut from crystal obtained from Marubeni Iida, Japan. Ultrasonic waves propagated along [110] direction, velocity measured by pulse-echo method. Room temperature density 6.85 gmcm^{-3}. T_N=522 K. Measured in air.
2	18	du Plessis, P. de V., van Tonder, S. J., and Alberts, L.	1971		5-700		Same as above.
3	18	du Plessis, P. de V., van Tonder, S. J., and Alberts, L.	1971		79-654		Same as above.
4	18	du Plessis, P. de V., van Tonder, S. J., and Alberts, L.	1971		82-653		Same as above.
5	58	Reichardt, W., Wagner, V., and Kress, W.	1975		293		Flame-grown crystals 3-4 cm^3 from Sitronix, Geneva and Koch-Light Laboratories, Colnbrook. Calculation from phonon dispersion curves obtained by inelastic neutron scattering. T_N=523 K. Measured in air at room temperature.
6	58	Reichardt, W., Wagner, V., and Kress, W.	1975		293		Same as above.
7	58	Reichardt, W., Wagner, V., and Kress, W.	1975		293		Same as above.
8	58	Reichardt, W., Wagner, V., and Kress, W.	1975		293		Same as above.
9	59	Uchida, N. and Saito, S.	1972		293		Single crystal plates 0.3-0.7 cm thick and 0.5-1.0 cm^2 in area. Grown by flame fusion by Nakazumi Crystals Corp., Osaka, Japan. Annealed at 1500°C for one day in air. Calculation from velocity data obtained by pulse-superposition method. T_N=523 K.
10	59	Uchida, N. and Saito, S.	1972		293		Same as above.
11	59	Uchida, N. and Saito, S.	1972		293		Same as above.
12	59	Uchida, N. and Saito, S.	1972		293		Same as above.
13	60	Coy, R. A., Thompson, C. W., and Gürmen, E.	1976		293		Single crystals of 2 cm^3 volume. Calculation from data obtained by coherent inelastic neutron diffraction.
14	60	Coy, R. A., Thompson, C. W., and Gürmen, E.	1976		293		Same as above.

TABLE 18. MEASUREMENT INFORMATION ON THE ELASTIC CONSTANTS OF NiO (continued)

Cur. No.	Ref. No.	Author(s)	Year	Method Used	Temp. Range, K	Name and Specimen Designation	Composition (weight percent), Specifications, and Remarks
15	60	Coy, R. A., Thompson, C. W., and Gürmen, E.	1976		293		Single crystals of 2 cm^3 volume. Calculation from data obtained by coherent inelastic neutron diffraction.
16	60	Coy, R. A., Thompson, C. W., and Gürmen, E.	1976		600		Same as above.
17	60	Coy, R. A., Thompson, C. W., and Gürmen, E.	1976		600		Same as above.
18	60	Coy, R. A., Thompson, C. W., and Gürmen, E.	1976		600		Same as above.

TABLE 19. TABULATION OF ELASTIC CONSTANT MEASUREMENTS OF NiO

[Temperature, T, K; Elastic Constants, C_{ij}, dynes/cm^{2}X10^{12}]

T	C_{ij}
CURVE 1 $\frac{1}{2}(C_{11}-C_{12})$	
60	0.450
118	0.456
158	0.471
198	0.498
237	0.542
278	0.601
317	0.690
357	0.799
396	0.899
437	0.994
474	1 051
494	1.073
515	1.094
519	1.163
526	1.273
534	1.333
594	1.345
655	1.345
CURVE 2 $\frac{1}{3}(C_{11}+2C_{12})$	
5	1.437
50	1.436
100	1.434
150	1.424
200	1.414
250	1.392
300	1.358
350	1.313
400	1.270
450	1.245
475	1.269
485	1.353
485	1.447
500	1.541
515	1.507
525	1.450
550	1.414
575	1.410
600	1.410
625	1.410
650	1.410
675	1.410
700	1.410

T	C_{ij}
CURVE 3 $\frac{1}{2}(C_{11}+C_{12}+2C_{44})$	
79	2.684
118	2.684
159	2.684
197	2.684
239	2.684
277	2.690
317	2.690
358	2.686
397	2.686
437	2.694
475	2.719
484	2.868
496	3.009
502	2.020
535	3.024
595	3.033
654	3.034
CURVE 4, C_{44}	
82	1.086
120	1.088
160	1.088
197	1.088
238	1.093
278	1.097
318	1.096
358	1.101
396	1.101
436	1.101
476	1.107
496	1.112
520	1.140
534	1.144
555	1.150
595	1.167
653	1.182
CURVE 5	
293	C_{11}=3.28
CURVE 6	
293	C_{12}=0.58

T	C_{ij}
CURVE 7	
293	C_{44}=1.07
CURVE 8	
293	$\frac{1}{3}(C_{11}+2C_{12})$=1.48
CURVE 9	
293	C_{11}=2.70
CURVE 10	
293	C_{12}=1.25
CURVE 11	
293	C_{44}=1.05
CURVE 12	
293	$\frac{1}{3}(C_{11}+2C_{12})$=1.75
CURVE 13	
293	C_{11}=5.031*
CURVE 14	
293	C_{12}=1.543
CURVE 15	
293	C_{44}=0.974
CURVE 16	
600	C_{11}=4.415*

T	C_{ij}
CURVE 17	
600	C_{12}=1.917
CURVE 18	
600	C_{44}=0.806

*Not shown in figure

TABLE 20

PROVISIONALLY RECOMMENDED VALUES FOR YOUNG'S MODULUS OF NiO IN THE RANGE 295-595 K

Temperature, K	Young's Modulus, 10^{11} dyne/cm^2
295	9.07
320	9.08
340	9.09
360	9.10
380	9.14
400	9.20
420	9.27
440	9.38
460	9.56
480	9.90
500	10.68
515	12.24
520	14.00
520	24.18
525	24.48
540	24.00
560	23.24
580	22.36
595	21.66

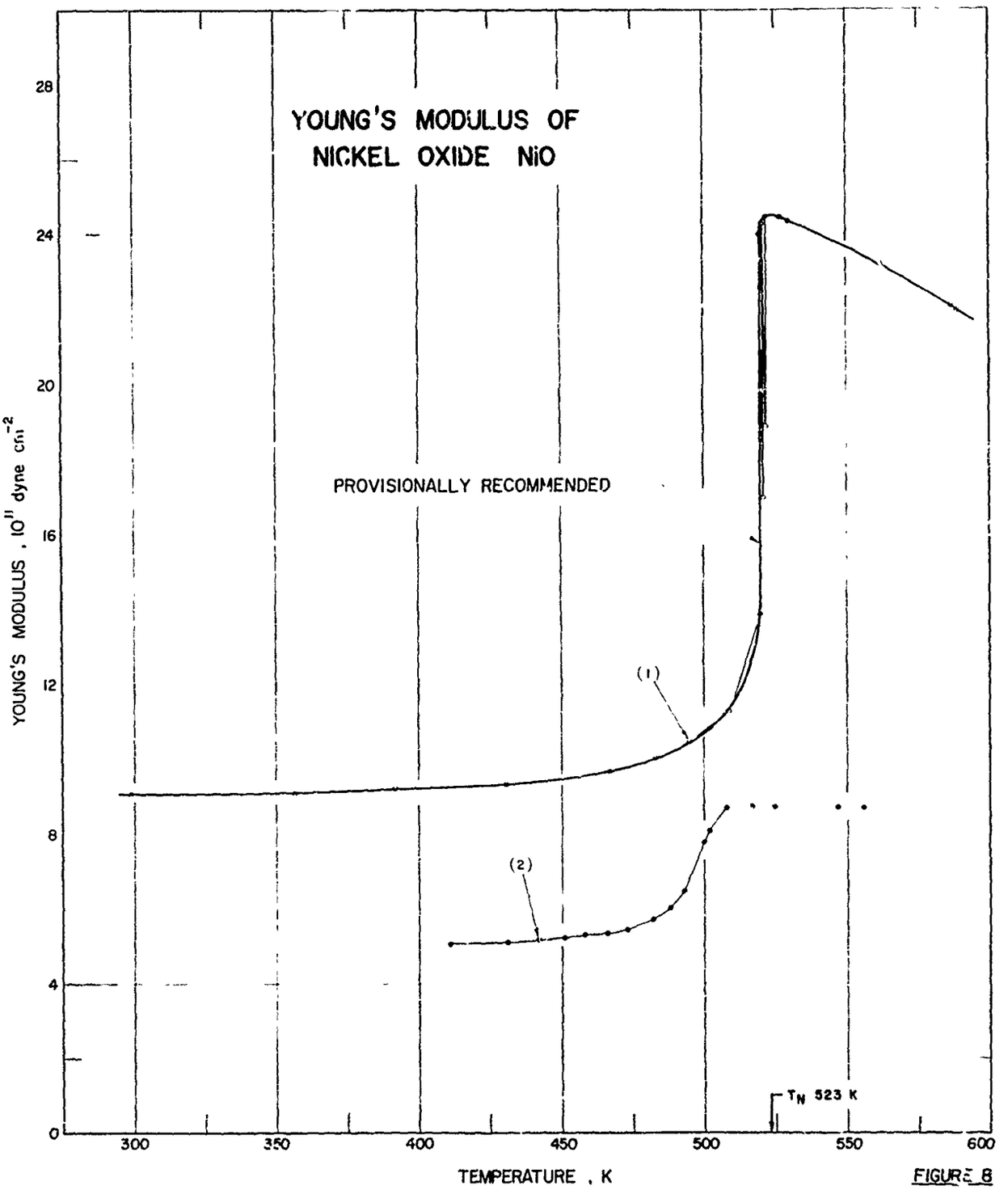
YOUNG'S MODULUS OF
NICKEL OXIDE NiO
PROVISIONALLY RECOMMENDED
YOUNG'S MODULUS , 10^{11} dyne cm^{-2}
TEMPERATURE , K
(1)
(2)
T_N 523 K
0
4
8
12
16
20
24
28
300
350
400
450
500
550
600

FIGURE 8

TABLE 21. MEASUREMENT INFORMATION ON YOUNG'S MODULUS OF NiO

Cur. No.	Ref. No.	Author(s)	Year	Method Used	Temp. Range, K	Name and Specimen Designation	Composition (weight percent), Specifications, and Remarks
1	25	Notis, M. R., Spriggs, R. M., and Hahn, W.C., Jr.	1973		299-589		Sintered. Rectangular bars. 99.999% pure NiO powder from Johnson-Matthey Co. Air fired at 1173 K for 10 h, ground, dried for 24 h at 413 K. Pressure-sintered at 10,000 psi and 1373 K for 90 min. Density 92.0-99.93 of x-ray density. T_N=523 K. Room temperature elastic moduli found by resonant sphere method. Young's modulus also determined by three-part composite oscillator method. Measured in air.
2	61	Street, R. and Lewis, B.	1951		411-556		Bars with square cross-section. Manufactured by Murex, Ltd. Longitudinal oscillations generated by quartz crystals cemented to bars. Measured by dynamic method.

TABLE 22. TABULATION OF MEASUREMENTS OF YOUNG'S MODULUS OF NiO

[Temperature, T, K; Young's Modulus, Y, dynes/cm^{2}X10^{11}]

T	Y
CURVE 1	
299.16	9.08
357.16	9.09
392.16	9.21
431.16	9.32
462.16	9.65
483.16	10.09
488.16	10.09*
495.16	10.46
509.16	11.28
520.16	13.86
511.16	16.95
512.16	18.88
520.16	24.00
521.16	24.30
522.16	24.45
527.16	24.45
530.16	24.33
562.16	23.20
587.16	22.11
589.11	21.94
CURVE 2	
411.56	5.06
431.86	5.13
442.16	5.18
451.26	5.23
458.36	5.30
402.36	5.35*
466.86	5.35
469.06	5.37*
473.16	5.44
475.16	5.49*
478.06	5.57*
480.06	5.65
482.36	5.72
484.56	5.80*
485.96	5.86*
487.06	5.93*
488.46	6.02
490.16	6.10*
491.26	6.23*
492.56	6.37*
493.26	6.47
494.36	6.56*

T	Y
CURVE 2 (cont.)	
495.36	6.67*
496.76	6.86*
498.36	7.24*
499.26	7.42*
500.16	7.67*
500.86	7.79
501.26	7.88*
501.56	8.00*
502.76	8.08
504.16	8.22*
506.06	8.45*
507.76	8.60*
508.86	8.70
510.66	8.74*
512.16	8.75*
517.36	8.74
525.76	8.73
532.86	8.72*
539.36	8.71*
547.36	8.70
556.46	8.69

*Not shown in figure

3.6 Thermal Expansion

The thermal properties of a crystal are generally characterized by the coefficients of thermal expansion of the material. These may be specified in two ways:

The instantaneous (linear) coefficient of thermal expansion is defined by

$$\alpha_I \equiv \frac{1}{\ell}\left(\frac{\partial \ell}{\partial T}\right)_p \tag{8}$$

where ℓ is the length of the specimen along a given direction and T the absolute temperature; as shown by the formula, the measurements are taken at constant pressure. The mean coefficient of thermal expansion is defined by

$$\alpha_M \equiv \frac{1}{\ell_o}\frac{\ell - \ell_o}{T - T_o} \tag{9}$$

where ℓ_o is the length of the specimen along a given direction at a reference temperature T_o, and ℓ is the length at some other absolute temperature T. It is common practice to set T_o = 298 K, i.e., to refer all measurements of ℓ to the prevailing value, ℓ_o, at room temperature. As is implied by the wording, Eq. (8) provides information concerning the expansion properties of the material at temperature T, whereas Eq. (9) represents a quantity which is averaged over the temperature range $|T - T_o|$.

As is well known, the coefficient of linear expansion is proportional to the molar heat capacity at constant volume, $\tilde{C}_V$, through the relation

$$\alpha_I = \gamma \tilde{C}_V / 3B\tilde{V} \tag{10}$$

where γ is the Grüneisen constant, B is the bulk modulus, and $\tilde{V}$ the molar volume of the solid. This proportionality is found to be quite well satisfied for cubic crystals.

The provisionally recommended values for both α_I and α_M are cited in Table 23. For $T \lesssim 600$ K, α_I was taken from Curve 2; while at higher temperatures α_I was calculated from the α_M values of Curve 4, by converting the data, represented by Eq. (9), so as to conform to Eq. (8). The two portions of the curve were smoothly joined in the region near 600 K. The recommended α_M values were then obtained by the inverse process of treating the recommended α_I curve, subject to Eq. (8), so as to assume the form demanded by Eq. (9) with $T_o = 298$ K.

The original data sets and the recommended values are plotted in Fig. 9. Measurement information for the determination of α_I or of α_M is provided in Table 24. The tabulation of the experimental data is shown in Table 25.

One should note that Curve 3 has been ignored in setting up the recommended curves. This was done on the basis that according to Eq. (10), α_I should follow the heat capacity anomaly, exhibited in Fig. 5, which is associated with magnetic ordering effects near 523 K. These effects show up in Curve 2 but not in Curve 3. Apparently, complications arise in the conversion of lattice parameter data to linear thermal expansion coefficients. Below the Néel point, NiO undergoes a rhombohedral distortion, so that it is not really correct to characterize the unit cell dimension by a lattice parameter appropriate to the cubic phase of NiO which prevails only above the Néel point. These difficulties are avoided in the direct dilatometric measurements reported in Refs. 17 and 46.

TABLE 23. PROVISIONALLY RECOMMENDED VALUES FOR MEAN AND INSTANTANEOUS COEFFICIENTS OF THERMAL EXPANSION OF NICKEL OXIDE NiO

Temperature, K	α, 10^{-6} K^{-1}		
	Instantaneous	$\Delta L/L_0$(%)	Mean
	A		
80	3.05	-0.1463	6.71
100	3.90	-0.1394	7.04
200	7.17	-0.0840	8.57
298	9.98	0.0000	—
300	10.04	0.0020	10.00
400	13.25	0.1184	11.61
420	13.96	0.1457	11.94
440	14.72	0.1743	12.27
460	15.54	0.2046	12.63
480	16.52	0.2367	13.01
500	17.80	0.2710	13.42
520	21.15	0.3100	13.96
525	21.90	0.3207	14.13
540	15.00	0.3484	14.40
560	13.78	0.3772	14.40
580	13.48	0.4044	14.34
600	13.35	0.4313	14.28
620	13.31	0.4579	14.22
640	13.35	0.4846	14.17
700	13.53	0.5652	14.06
800	13.86	0.7022	13.99
900	14.25	0.8427	14.00
1000	14.71	0.9875	14.07
1100	15.21	1.1371	14.18
1200	15.75	1.2919	14.32
1300	16.48	1.4531	14.50
1400	17.00	1.6205	14.70
1500	17.88	1.7949	14.93
1600	18.52	1.9769	15.18
1700	19.35	2.1662	15.45
1800	20.20	2.3640	15.74
1900	21.15	2.5707	16.05
2000	22.14	2.7872	16.38
2100	22.98	3.0128	16.72
2200	24.28	3.2491	17.08

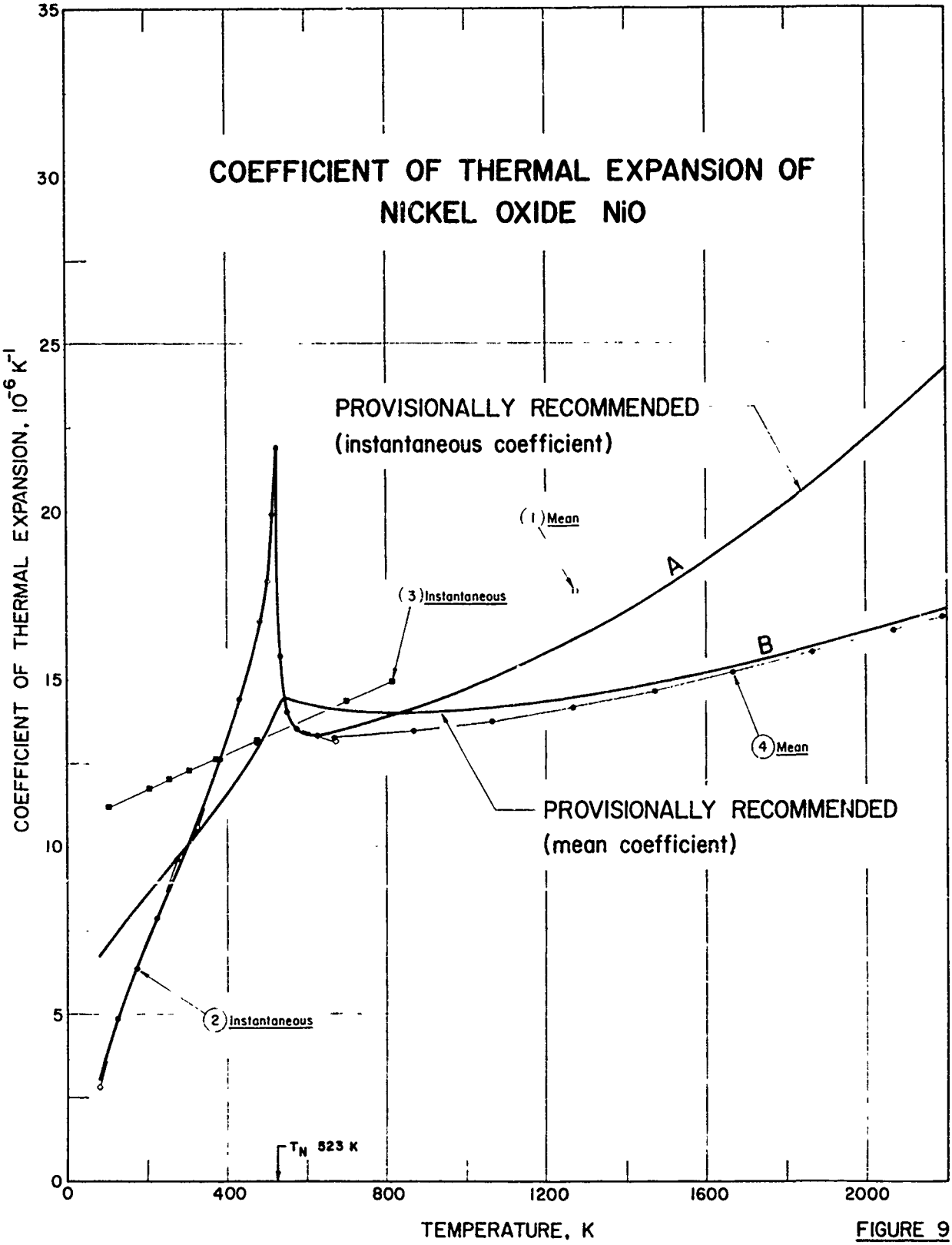
COEFFICIENT OF THERMAL EXPANSION OF
NICKEL OXIDE NiO
COEFFICIENT OF THERMAL EXPANSION, 10^{-6} K^{-1}
TEMPERATURE, K
PROVISIONALLY RECOMMENDED
(instantaneous coefficient)
(1) Mean
(3) Instantaneous
A
B
(4) Mean
PROVISIONALLY RECOMMENDED
(mean coefficient)
(2) Instantaneous
T_N 523 K
0
5
10
15
20
25
30
35
0
400
800
1200
1600
2000

FIGURE 9

TABLE 24. MEASUREMENT INFORMATION ON THE COEFFICIENT OF THERMAL EXPANSION OF NiO

Cur. No.	Ref. No.	Author(s)	Year	Method Used	Temp. Range, K	Name and Specimen Designation	Composition (weight percent), Specifications, and Remarks
1	62	Tylecote, R. F.	1960		1273	Ni/NiO	NiO compressed to 24.3 tons/in^2, sintered at 1400°C for 20 h in air; 83.5% of theoretical density achieved. Dilatometer measurement of mean coefficient of thermal expansion.
2	17 46	Foëx, M. Foëx, M.	1948 1952		80-650		Calcination of $Ni(NO_3)_2$ in air, followed by compression at 3 tons/cm^2. Dilatometer measurements of instantaneous coefficients of thermal expansion.
3	63	Srivasta, S. P., Srivasta R. C., Singh, I. D., Pandey, S. D., and Gupta, P. L.	1977		105-813		X-Ray measurements on unspecified NiO sample, from which instantaneous coefficients of thermal expansion were calculated.
4	64	Nielsen, T. H. and Leipold, M. H.			472-2190		$NiSO_4$ calcined at 900°C for 20 hours, then hot pressed to greater than 95% of theoretical density at 10,000 psi for 90 min. at 1000°C. Sample subsequently heated to 1800°C in 95% O_2 - 5% N_2 atmospheres for 1 hour. Dilatometer measurements up to 1000°C, optical measurements up to 1930°C of the mean coefficient of thermal expansion.

TABLE 25. TABULATION OF MEASURED COEFFICIENT OF THERMAL EXPANSION OF NiO

[Temperature, T, K; Thermal Coefficient of Expansion, α_M(mean) or α_I (instantaneous), 10^{-6} K^{-1}]

T	α
Curve 1 (Mean)	
1273	17.1
Curve 2 (Instantaneous)	
80	2.82
125	4.87
174	6.36
224	7.86
27o	9.64
323	10.56
382	12.63
430	14.40
483	16.75
501	17.91
515	19.90
524	21.89
531	15.70
550	14.04
575	13.52
626	13.33
674	13.13
Curve 3 (Instantaneous)	
105	11.23
205	11.75
254	12.01
305	12.28
373	12.64
473	13.16
700	14.35
813	14.93
Curve 4 (Mean)	
472	13.11
669	13.22
867	13.43
1064	13.72
1268	14.14
1472	14.63
1669	15.19
1866	15.79
2070	16.42
2190	16.81

4. REFERENCES

1. Brownlee, L. D. and Mitchell, E. W. J., Proc. Phys. Soc. (London) B65, 710-716 (1952).
2. Roth, W. L., Phys. Rev. 110, 1333-1341 (1958); 111, 772-781 (1958).
3. Alberts, L. and Lee, E. W., Proc. Phys. Soc. (London) 78, 728-733 (1961).
4. Keem, J. E., Thesis, Purdue University, West Lafayette, IN, 1976 (unpublished).
5. Nakazumi, Y., Nakazumi Crystals Corp., Kobe, Japan.
6. Okada, T., Matsumi, K., and Makino, H., Solid State Phys. (Japan) 6, 170-175 (1971).
7. Clausen, E. M. and Rutter, J. W., General Electric Research Laboratory Report, Schenectady, NY, 1964.
8. Sakurai, T. and Ishigame, M., J. Cryst. Growth 2, 284-286 (1968). Sakurai, T., Kamada, O., and Ishigame, M., J. Cryst. Growth 2, 326-327 (1968).
9. Eklund, P. C., J. Crystal Growth 16, 271-273 (1972).
10. Cech, R. E. and Allessandrini, E. I., Trans. ASM 51, 56 (1959).
11. Kurosawa, K., Saito, S., and Takemoto, T., Japanese J. Appl. Phys. 11, 1230 (1972); 14, 887-888 (1975).
12. Hill, G. J. and Wanklyn, B. M., J. Cryst. Growth 3/4, 475-479 (1968).
13. Osburn, C. M. and Vest, R. W., J. Phys. Chem. Solids 32, 1355-1363 (1971).
14. Keem, J. E., Chem. Instr. 6, 133-141 (1975).
15. Harman, T. C. and Honig, J. M., "Thermoelectric and Thermomagnetic Effects and Applications" (McGraw-Hill, New York, 1967), Chap. I.
16. Herring, C., in Semiconductors and Phosphors, Schön, M. and Welker, H. M., eds. (Vieweg, Braunschweig, 1956), p. 184-235.
17. Foëx, M., Compt. rend. Acad. Sci. (Paris) 227, 193-194 (1948).

18. Du Plessis, P. de V., van Tonder, S. J., and Alberts, L., J. Phys. C. Solid State Phys. 4, 1983-1987 (1971).

19. Guggenheim, E. A., "Thermodynamics, an Advanced Treatment for Chemists and Physicists" (North-Holland, Amsterdam, 1950), Chap. 8.

20. Lewis, F. B. and Saunders, N. H., J. Phys. C. Solid State Phys. 6, 2525-2532 (1973).

21. Heikes, R. R. and Ure, R. W., "Thermoelectricity: Science and Engineering" (Interscience, New York, 1961), Chap. 4.

22. Keem, J. E., Honig, J. M., and Van Zandt, L. L., in "Valence Instabilities and Related Narrow-Band Phenomena," Parks, R. D., ed. (Plenum, New York, 1977), p. 551-554.

23. Emin, D. and Holstein, T., Ann. Phys. (NY) 53, 439-520 (1969). Friedman, L. and Holstein, T., Ann. Phys. (NY) 21, 494-549 (1963). Emin, D., Ann. Phys. (NY) 64, 336-395 (1971).

24. Kim, K. S. and Winograd, N., Surf. Sci. 43, 625-643 (1974).

25. Notis, M. R., Spriggs, R. M., Hahn, Jr., W. G., J. Appl. Phys. 44, 4165-4171 (1973).

26. Emin, D., in "Physics of Structurally Disordered Solids," S. S. Mitra, ed. (Plenum, New York, 1976), pp. 461-505.

27. Rosenberg, H. M., "Low Temperature Solid State Physics" (Clarendon, Oxford, 1963), Chap. 3.

28. Parravano, G., J. Chem. Phys. 23, 5-10 (1955).

29. Austin, I. G., Springthorpe, A. J., Smith, B. A., and Turner, C. E., Proc. Phys. Soc. (London), 90, 157-174 (1967).

30. Friedman, F., Weichman, F. L., and Tannhauser, D., Phys. Stat. Solidi (a)27, 273-279 (1975).

31. Ksendzov, Ya. M. and Drabkin, I. A., Fiz. Tverd. Tela 7, 1884-1886 (1965) [Soviet Phys.--Solid State 7, 1519-1520 (1965)].

32. Koide, S., J. Phys. Soc. Japan 20, 123-132 (1965).

33. Morin, F. J., Phys. Rev. 93, 1199-1204 (1954).

34. Yamaka, E. and Sawamoto, K., Phys. Rev. 112, 1861-1862 (1958).

35. Vernon, M. W. and Lovell, M. C., J. Phys. Chem. Solids 27, 1125-1131 (1966).

36. Aiken, J. G. and Jordan, A. G., J. Phys. Chem. Solids 29, 2153-2167 (1968).

37. Zhuze, V. P. and Shelykh, A. I., Fiz. Tverd. Tela 5, 1756-1759 (1963) [Soviet Phys.--Solid State 5, 1278-1280 (1963)].

38. van Daal, H. J. and Bosman, A. J., Phys. Rev. 158, 736-747 (1967).

39. Nowotny, J. and Wagner, Jr., J. B., Bull. Acad. Polon. Sci., Sér. Sci. Chim. 21, 931-936 (1973).

40. Melik-Davtyan, R. L., Shvartsenau, N. F., and Shelykh, A. I., Izv. Akad. Nauk. SSSR, Neorgan. Mat. 2, 21-31 (1966) [Inorg. Mater. 2, 16-24 (1966)].

41. van Houten, S., J. Phys. Chem. Solids 17, 7-17 (1960).

42. Nachman, M., Cojocaru, L. N., and Rîbco, L. V., Phys. Stat. Solidi 8, 773-783 (1965).

43. Shimomura, Y. and Tsubokawa, I., J. Phys. Soc. Jap. 9, 19-21 (1954).

44. Cimino, A., Molinari, E., and Romeo, G., Zeits. Phys. Chem. (Frankfurt) 16, 101-125 (1958).

45. Wright, R. W. and Andrews, J. P., Proc. Phys. Soc. (London) A62, 446-455 (1947).

46. Foëx, M., Bull. Soc. Chim. (France) 5th Ser., 373-379 (1952).

47. von Baumbach, H. H. and Wagner, C., Z. Phys. Chem. B24, 59-67 (1933).

48. Schlosser, E. G., Z. Elektrochem. 65, 453-462 (1961).

49. Dereń, J. and Ziółkowski, J., Bull. Acad. Polon. Sci., Sér. Sci. Chim. 14, 443-448 (1966).

50. Seltz, H., DeWitt, B. J., and McDonald, H. J., J. Am. Chem. Soc. 62, 88-89 (1940); 62, 3527 (1940).

51. Tomlinson, J. R., Domash, L., Hay, R. G., and Montgomery, C. W., J. Am. Chem. Soc. 77, 909-910 (1955).

52. King, E. G., J. Am. Chem. Soc. 79, 2399-2400 (1957).

53. Zhuze, V. P., Novruzov, O. N., and Shelykh, A. I., Fiz. Tverd. Tela 11, 1287-1296 (1969) [Soviet Phys.--Solid State 11, 1044-1051 (1970)].

54. White, H. W., J. Chem. Phys. 61, 4907-4909 (1974).

55. Shchelkotunov, V. A. and Danilov, V. N., Izv. Akad. Nauk. SSSR, Ser. Fiz. 35, 1158-1162 (1971).

56. Kingery, W. B., Francl, J., Cobe, R. L., and Vasilos, T., Jour. Am. Cer. Soc. 37, 107-110 (1954).

57. Slack, G. A. and Newman, R., Phys. Rev. Lett. 1, 359-360 (1958).

58. Reichardt, W., Wagner, V., and Kress, W., J. Phys. C. Solid State Phys. 8, 3955-3962 (1975).

59. Uchida, N. and Saito, S., J. Acous. Soc. America 51, 1602-1605 (1972).

60. Coy, R. A., Thompson, C. W., and Gürmen, E., Solid State Comm. 18, 845-847 (1976).

61. Street, R. and Lewis, B., Nature 168, 1036-1037 (1951).

62. Tylecote, R. F., J. Iron and Steel Inst. 196, 135-141 (1960).

63. Srivasta, S. P., Srivasta, R. C., Singh, I. D., Pandey, S. D., and Gupta, P. L., J. Phys. Soc. Japan 43, 885-890 (1977).

64. Nielsen, T. H. and Leipold, M. H., J. Amer. Ceram. Soc. 48, 164 (1965).